Mon. Not. R. Astron. Soc. **262**, 401–428 (1993)

# Two-integral distribution functions for axisymmetric galaxies

C. Hunter[1,2] and Edward Qian[1]

[1] *Department of Mathematics, Florida State University, Tallahassee, Florida 32306-3027, USA*
[2] *Sterrewacht, Huygens Laboratorium, Postbus 9513, 2300 RA Leiden, The Netherlands*

Accepted 1992 November 2. Received 1992 October 13

**ABSTRACT**

We present a new method for finding distribution functions, which depend only on the classical integrals of energy and angular momentum, for stellar systems with known axisymmetric densities. Our method is the analogue for the axisymmetric case of Eddington's classical solution for the isotropic distribution function, depending only on energy, of a known spherical density. Like his method, ours requires that the density be expressed as a function of the potential, and now also of a radial coordinate. Our solution is also an integral which is derived directly from the density, and hence can be used with complicated densities. Unlike Eddington's solution, ours is a contour integral. A numerical quadrature is generally required to evaluate this solution, but contour integrals can be computed accurately by numerical quadrature. This is a simpler and much more accurate procedure than direct solution of the integral equation for the distribution function, and is even preferable to an explicit evaluation if the latter is an infinite series, such as is obtained using Fricke's method. We give several examples, including some for which our distribution functions are new. Our method can be extended simply to the related problems of finding anisotropic distribution functions for spherical or disc systems.

**Key words:** celestial mechanics, stellar dynamics – galaxies: elliptical and lenticular, cD – galaxies: kinematics and dynamics.

## 1 INTRODUCTION

The most straightforward way of constructing self-consistent stellar systems is to start with an assumed potential. This potential defines both the self-consistent mass density $\rho$ of the system, and the families of orbits that can lie within it. The orbits are the building blocks from which the system is constructed. Binney & Tremaine (1987) call this the 'from $\rho$ to $f$' approach for finding a self-consistent distribution function $f$. Its simplest instance is that of finding an isotropic distribution function, depending only on the energy $E$, for a specified spherical density field. Eddington (1916) showed that this can be done by first expressing the density as a function of the potential $\Psi$, and then solving an Abel integral equation. The analogous problem of finding a two-integral distribution function, depending on the two classical integrals of the energy $E$ and the component $J$ of angular momentum about the axis of symmetry, for a specified axisymmetric density distribution, has proved to be more difficult. It is this problem with which we shall primarily be concerned, although we recognize that it is now well known that third integrals generally play an important role in the dynamics of axisymmetric galaxies (de Zeeuw 1987).

The mathematical problem is that of solving either the integral equation (2.1) or its simple-looking alternative form (equation 2.6). Like the integral equation solved by Eddington (1916) for the spherical case, these are integral equations of the first kind, in which the unknown distribution function $f$ occurs inside the integral only. A well-known feature of such equations is that the unknown function is generally less well behaved than the known function outside the integral (Courant & Hilbert 1953), here the density $\rho$, from which it is to be obtained. This feature appears in Eddington's solution (see equation 3.2), in which two differentiations of the density are needed to compute $f$. There are strong indications that the requirements necessary for the solution of the axisymmetric problem are considerably more stringent, although they are still not fully understood. Some degree of analyticity of the density $\rho$ has been a necessary ingredient in all the solutions obtained so far, such as for the validity of the series expansions needed to implement Fricke's (1952) method. Dejonghe (1986, section 1.2) gives a vivid example of how well behaved a density can be, relative to the distribution function that generates it, in the form of a discontinuous $f$ which generates

an infinitely smooth $\rho$. We give an even more extreme example in Appendix D of an $f$ with a delta function which also generates an infinitely smooth $\rho$.

Fricke (1952) took the first major step towards the solution of the axisymmetric problem. He showed that distribution functions which are products $E^j J^{2k}$ of the two integrals of motion correspond to densities which are proportional to products $\Psi^{j+k+(3/2)} R^{2k}$ of the potential $\Psi$ and the radial distance $R$ from the axis of symmetry. Such elementary solutions with different values of the powers $j$ and $k$ can be combined. Most of the disappointingly few analytical distribution functions that have been obtained to date in a 'from $\rho$ to $f$' approach are finite sums (Lynden-Bell 1962; Lake 1981), infinite sums (Hunter 1975; Dejonghe 1986) or infinite sums of infinite sums (Nagai & Miyamoto 1976; Dejonghe 1986; Dejonghe & de Zeeuw 1988; Evans, de Zeeuw & Lynden-Bell 1990) of his solutions. They are obtained by first expressing the density as a function $\rho(\Psi, R^2)$, and then expanding $\rho$ as a power series.

The second major step towards the solution of the axisymmetric problem was Lynden-Bell's (1962) introduction of integral transform techniques. He used a Laplace transform, and showed formally that $f$ can be obtained by carrying out *two* inverse Laplace transforms of a function containing a Laplace transform of the density $\rho$. This work gave the first clear indication of two major snags. One is that of the stringent conditions that must be imposed on the density if a distribution function is to be found for it, because it is possible to perform two inverse Laplace transforms on a function obtained from a single Laplace transform only for a restricted class of well-behaved density functions. The other is that density information at complex values of the arguments is needed to implement the method, information that observations do not, of course, provide (Binney & Tremaine 1987, section 4.5.2). Both of these snags have recurred in later work. Hunter (1975) showed that Lynden-Bell's double Laplace transform inversion is equivalent to the inversion of a Stieltjes transform, which requires an analytic continuation of the density to complex arguments, and also imposes conditions on $\rho$ that may not be met even in cases for which the physical problem has a solution. Dejonghe (1986) used a combined Laplace–Mellin transform (Laplace in energy $E$ and potential $\Psi$, and Mellin in angular momentum $J$ and radial distance $R$), but he too encountered the same difficulty of requiring an analytic continuation of the density to complex arguments. Geigant (1991) has recently proved a rigorous existence theorem for the closely related problem for an anisotropic spherical system. Her work, like Lynden-Bell's, is based on Laplace transforms and her existence theorem requires, as does Hunter's Stieltjes transform solution, that the density be holomorphic throughout the complex $R^2$-plane except for its negative real axis.

The integral transform methods operate on values of $\rho$ and $f$ outside their physically relevant domains, which occupy only parts of the $(\Psi, R^2)$- and $(E, J^2)$-planes respectively. We believe that this feature has been insufficiently appreciated in previous work, and that it is a source of difficulties which are most easily overcome by our new solution. For instance, the density $\rho(\Psi, R^2)$ in the example illustrated in Fig. 3(a) (see later) has singularities in the non-physical regions of $(\Psi, R^2)$-space which preclude the existence of its integral transforms. The restricted forms of the physically relevant domains of $\rho$ and $f$, which are delineated in Section 2, play a fundamental role in our solution. Our solution does require an analytical continuation of the density $\rho$ to complex arguments to give meaning to its contour integral form, but some of the restrictions inherent in earlier methods are relaxed. The integrand of the contour integral is derived directly from $\rho$ and can have singularities, including branch points. The way in which the contour of integration is drawn relative to these singularities and the question of which branch of the integrand to evaluate are crucial, so we discuss these points carefully.

After the formulation of our problem in Section 2, we state our contour integral solution, without derivation, in the first part of Section 3. Section 3 forms the essential core of the paper. We illustrate our method of solution in Section 3.2 with a detailed account of its application to the model of Kuzmin & Kutuzov (1962). This example illustrates the general types of singularity that occur. We describe and classify them in Section 3.3. We then justify our contour integral solution in Section 3.4, where we verify that it does indeed satisfy the fundamental integral equation. Having put our solution on a firm footing, we use it to derive two new distribution functions in Section 4, one for the flattened isochrone of Evans, de Zeeuw & Lynden-Bell (1990) and the other for a model due to Satoh (1980). The work up to this stage is restricted to systems of finite total mass. We show in Section 5 that our contour integral solution can readily be adapted to cases of infinite total mass for which the range of the potential is infinite. Section 6 summarizes our results and presents our conclusions.

To make the presentation as direct as possible, we have deferred the discussion of several important aspects of our method of solution to appendices. Appendix A relates Fricke's (1952) expansion method to our method. Appendix B relates our method to integral transform methods that have been used in the past. Appendix C shows how our method can be applied to the closely related problems of finding anisotropic distribution functions for spherical and disc-like stellar systems. Appendix D gives the example described earlier, in which our contour integral solution recovers an $f$ with a delta function from the analytic density that it generates.

## 2 FORMULATION

We give the fundamental integral equation in Section 2.1, and an alternative version of it in Section 2.3. Section 2.2 discusses the physically relevant domains $\boldsymbol{P}$ and $\boldsymbol{P}^*$ of the density $\rho$ in $(\Psi, R^2)$- and $(\Psi, R^2\Psi)$-spaces respectively, and the domain $\boldsymbol{F}$ of the unknown distribution function $f$ in $(E, J^2)$-space.

### 2.1 The fundamental integral equation

We use cylindrical polar coordinates $(R, \phi, z)$ for the axisymmetric system, with the $z$-axis being that of symmetry, and $J = Rv_\phi$ being the component of angular momentum about it. We consider a system of infinite extent, but of a finite total mass $M$. It is well known that a given density determines only the part of the distribution function that is even in $J$, which we shall write as $f(E, J^2)$. Following Binney & Tremaine (1987, chapter 4), we work with a positive gravitational potential $\Psi$ which tends to zero at large distances, and a relative energy $E = \Psi - (1/2)(v_R^2 + v_\phi^2 + v_z^2)$. The density that is obtained from integrating the distribution function $f(E, J^2)$ over velocity space is

$$\rho = \frac{2\pi}{R}\int_0^{\Psi} dE \int_0^{2R^2(\Psi - E)} \frac{f(E, J^2)}{\sqrt{J^2}}\, dJ^2 = \frac{2\pi}{R}\int_0^{2R^2\Psi} \frac{dJ^2}{\sqrt{J^2}} \int_0^{\Psi - (J^2/2R^2)} f(E, J^2)\, dE. \tag{2.1}$$

The integration in the $(E, J^2)$-plane is over the triangular region that is enclosed between the axes and the line

$$J^2 = 2R^2(\Psi - E), \tag{2.2}$$

as shown in Fig. 1(a), which is a variant of a figure first plotted by Lindblad (1934).

### 2.2 The domains *P*, *P**, and *F* of the fundamental integral equation

The density (equation 2.1), from which we are seeking to recover $f$, is represented in terms of the variables $R^2$ and $\Psi$, rather than the polar coordinates $R$ and $z$. Hence we need to consider whether $R^2$ and $\Psi$ can serve as independent variables. We shall restrict attention to gravitational potentials $\Psi(R^2, z^2)$ which are symmetric with respect to the equatorial plane. Provided that $\Psi$ decreases monotonically with increasing $z^2$ for fixed $R^2$, as is the case for centrally condensed objects such as that illustrated in Fig. 2, $z^2$ is determined uniquely when an $R^2$ and a value of $\Psi$, which does not exceed the potential $\Psi(R^2, 0)$ in the equatorial plane, are specified. Hence $R^2$ and $\Psi$ can serve as independent variables, and a unique representation of the form $\rho(\Psi, R^2)$ is obtained from a physical density field $\rho(R^2, z^2)$. The domain $\boldsymbol{P}$ of the density $\rho(\Psi, R^2)$ occupies that part of the $(\Psi, R^2)$-plane which lies to the left of a boundary, the thick full curve in Fig. 3(a), given by the equatorial potential $\Psi(R^2, 0)$. The shape of this boundary in Fig. 3(a) is typical of a case in which the central potential $\Psi(0, 0)$ is finite, and for which the potential $\Psi(R^2, z^2)$ also decreases monotonically with increasing $R^2$ for fixed $z^2$ so that the potential is largest at the centre. The finiteness of the total mass $M$ implies that the potential $\Psi \sim GM/\sqrt{R^2 + z^2}$ at large distances, so that the product $R\Psi$ remains bounded. This product generally achieves its largest value of $GM$ as $R \to \infty$ in the equatorial plane. For simplicity, we shall work throughout with units for which

$$GM = 1, \qquad \Psi(0, 0) = 1. \tag{2.3}$$

We shall label as $\boldsymbol{P^*}$ the domain of the density in the $(\Psi, R^2\Psi)$-plane, which is significant in view of the role that these coordinates play in equation (2.2) and Fig. 1(a). We plot this domain in Fig. 3(b). Its right-hand boundary also corresponds to points in the equatorial plane, and is concave upward because of the positivity of the relative energy of circular orbits in this

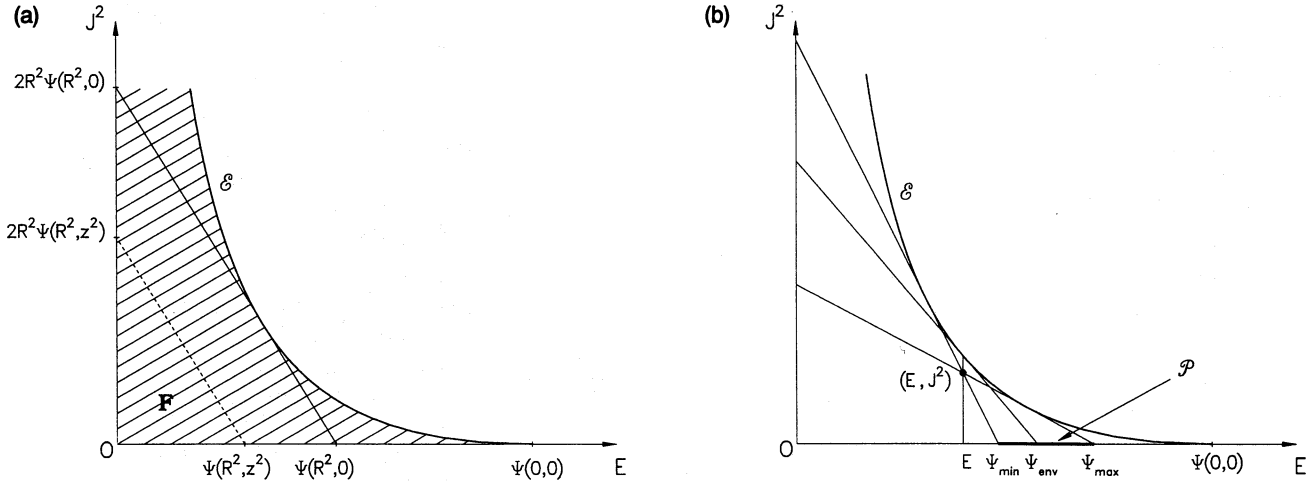


**Figure 1.** The domain $\boldsymbol{F}$ (shaded area) of bound orbits in $(E, J^2)$-space. A point in physical space, with coordinates $\Psi$ and $R^2$, is visited by the orbits for which the integrals lie in the triangle whose hypotenuse is given by equation (2.2). (a) shows both a general case (dashed line) and the extreme case (solid line) which occurs for a point in the equatorial plane $z = 0$. The extreme lines form the envelope $\mathscr{E}$. (b) focuses on a specific point of $\boldsymbol{F}$, and shows the three lines (2.2) which are related to it and are tangent to $\mathscr{E}$, as discussed in Section 2.2 of the text.

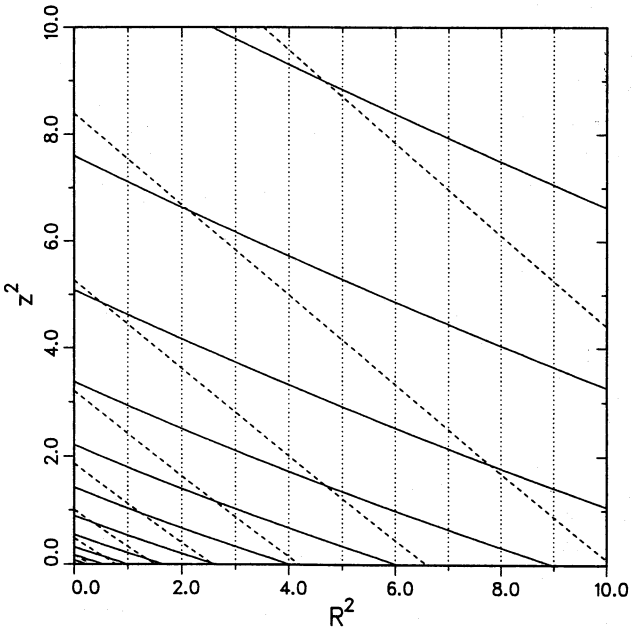


**Figure 2.** The equipotentials (dashed curves) and equidensity contours (solid curves) for an oblate $c/a=0.5$ Kuzmin–Kutuzov model (discussed in Section 3.2). Successive contour levels differ by constant factors (1.2 for potentials, $1.2^4$ for densities). Equipotentials are rounder than equidensity contours, which is why they are inclined more closely to 45°. Equidensity contours would slope more steeply than the equipotentials for a prolate model, rather than less steeply as here. The dashed curves and the dotted curves of constant $R$ form the coordinate grid for $\rho(\Psi, R^2)$ that is used in our analysis.

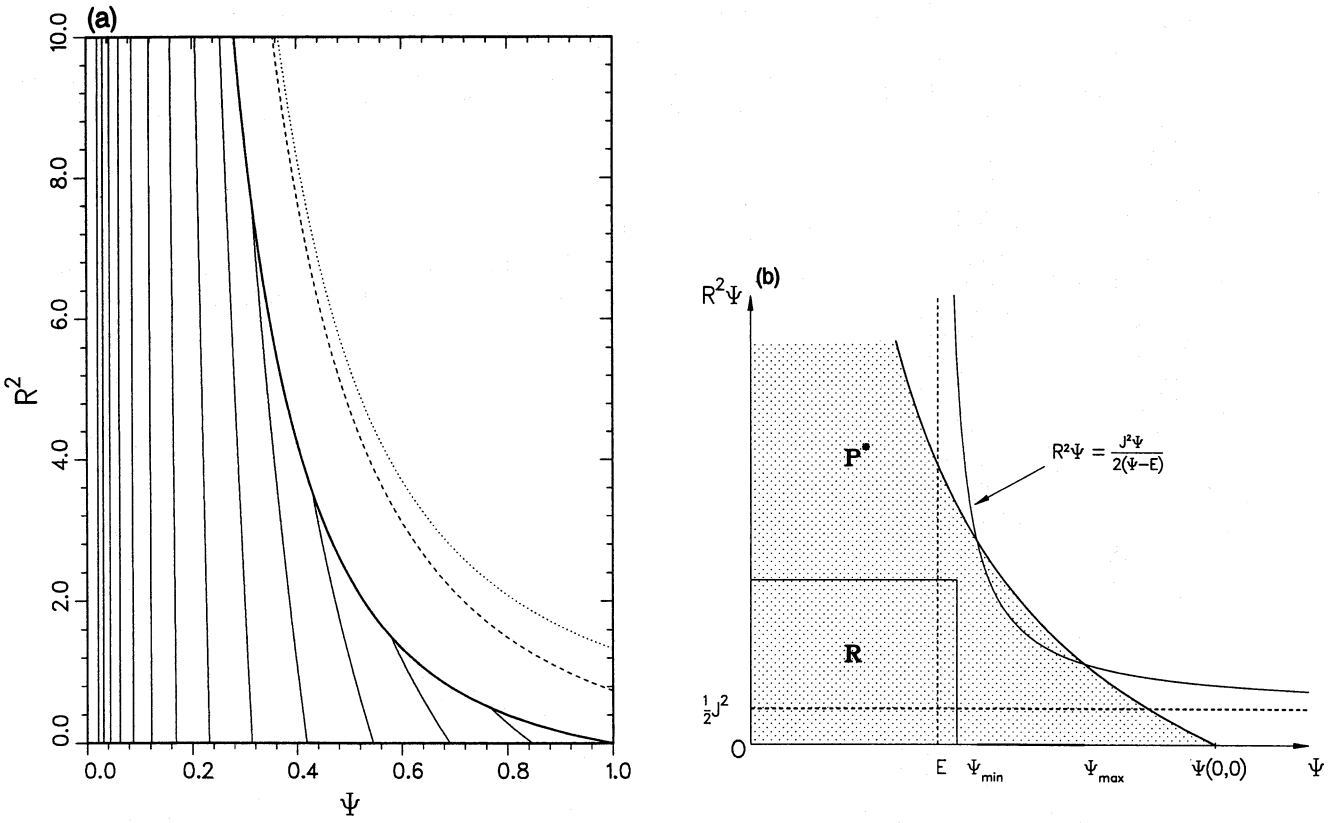


**Figure 3.** (a) The thin solid curves are equidensity curves within the physical domain $\boldsymbol{P}$ of the density. Successive contour levels differ by factors of 0.25. Outside $\boldsymbol{P}$, $\rho$ is infinite on the dashed curve, and complex to the right of the dotted curve. Like Fig. 2, this figure is plotted for an oblate $c/a=0.5$ Kuzmin–Kutuzov model. (b) The physically relevant domain $\boldsymbol{P}^*$ (dotted area) in $(\Psi, R^2\Psi)$-space. Equation (2.2), plotted for specific values of $E$ and $J^2$, is now a rectangular hyperbola, with the dashed asymptotes, and lies only partly in $\boldsymbol{P}^*$. The placement of the rectangle $\boldsymbol{R}$, which is used in the discussion of Section 3.4, is subject only to the requirement that its upper right corner lie in $\boldsymbol{P}^*$.

plane (see equation 2.4 below). The boundary asymptotes to the rectangular hyperbola $\Psi^2R^2=1$ at large distances where $\Psi(R^2, 0)\sim 1/R$.

The form of the domain $\boldsymbol{P}^*$ determines the form of the domain $\boldsymbol{F}$ of the $(E, J^2)$-plane for which a distribution function is needed. The latter region represents the totality of all the orbits that are bound in the given potential, and which contribute to the physical density. Geometrically, it is the union of the areas of all the triangles over which the integral (2.1) is evaluated. It is therefore the region enclosed between the $E$- and $J^2$-axes and the envelope $\mathscr{E}$ that is formed by the extreme lines of the form (2.2). The extreme lines are those for which the potential has its maximum equatorial-plane value of $\Psi(R^2, 0)$ (see Fig. 1a). The envelope $\mathscr{E}$ corresponds to circular orbits in this equatorial plane, and is given parametrically by

$$E=\Psi(R^2, 0)+R^2\frac{\mathrm{d}\Psi(R^2, 0)}{\mathrm{d}R^2}, \qquad J^2=-2R^4\frac{\mathrm{d}\Psi(R^2, 0)}{\mathrm{d}R^2}. \tag{2.4}$$

Its slope $-2R^2$ becomes steeper as the parameter $R^2$ increases upwards, and $\mathscr{E}$ asymptotes to the rectangular hyperbola $2EJ^2=1$ as $J^2\to\infty$.

Our aim is to recover $f(E, J^2)$ from $\rho$, and so we need to fix attention on one specific pair of values of the integrals $E$ and $J^2$. Orbits with these integrals are confined by the inequality

$$\Psi-E-\frac{J^2}{2R^2}=\frac{1}{2}(v_R^2+v_z^2)\geq 0 \tag{2.5}$$

and so contribute to the density $\rho(\Psi, R^2)$ at all $(\Psi, R^2\Psi)$ points for which the point $(E, J^2)$ lies within the triangles shown in Fig. 1(a). The relevant points of $\boldsymbol{P}^*$ lie on and above the rectangular hyperbola shown in Fig. 3(b). Their range in $\Psi$ is limited to $[\Psi_{\min}(E, J^2), \Psi_{\max}(E, J^2)]$, the limits appearing in Fig. 1(b) as the intercepts with the $E$-axis of the two lines (2.2) that pass through $(E, J^2)$ *and* also touch the envelope $\mathscr{E}$, these lines arising from extreme cases of triangles of $\boldsymbol{F}$ which include $(E, J^2)$. The triangle whose upper boundary is the tangent to $\mathscr{E}$ at $E$ also includes $(E, J^2)$, and the intercept $\Psi_{\mathrm{env}}(E)$ of this tangent with the $E$-axis lies between $\Psi_{\min}$ and $\Psi_{\max}$. The interval $(\Psi_{\min}, \Psi_{\max})$ shrinks to the single point $\Psi_{\mathrm{env}}(E)$ for a circular orbit.

When $R\Psi(R^2, 0)$ is an increasing function of $R^2$, as it is for the three models discussed in detail in Sections 3 and 4, then the first of equations (2.4) shows that $\Psi_{\mathrm{env}}(E)<2E$.

### 2.3 An alternative form of the fundamental integral equation

After switching to the representation $\rho(\Psi, R^2)$ for the density, equation (2.1) can be differentiated partially with respect to $\Psi$ to give the simpler integral equation

$$\frac{\partial\rho(\Psi, R^2)}{\partial\Psi}=2\sqrt{2}\pi\int_0^{\Psi}\frac{f[E, 2R^2(\Psi-E)]}{\sqrt{\Psi-E}}\,\mathrm{d}E. \tag{2.6}$$

The right-hand-side integral now involves values of $f$ along the bounding line (2.2) of the triangle of Fig. 1(a) only. Consequently, the value of $f$ for a specific $(E, J^2)$ point of $\boldsymbol{F}$ influences the value of $\partial\rho(\Psi, R^2)/\partial\Psi$ only at points of $\boldsymbol{P}^*$ that lie also on the curve $R^2\Psi=J^2\Psi/2(\Psi-E)$. This curve intersects the boundary of $\boldsymbol{P}^*$ at $\Psi=\Psi_{\min}(E, J^2)$ and $\Psi=\Psi_{\max}(E, J^2)$ (see Fig. 3b), and lies within $\boldsymbol{P}^*$ only between these points. A real solution to the present inversion problem would require $f$ to be recovered from the $\partial\rho/\partial\Psi$ values along this segment of the curve.

## 3 THE CONTOUR INTEGRAL SOLUTION

We state our contour integral solution in Section 3.1, where we also show that Eddington's (1916) solution can be obtained from it as a special case. We show in detail how to use our solution in Section 3.2, where we apply it to the Kuzmin–Kutuzov (1962) model, for which Dejonghe & de Zeeuw (1988) have already given a two-integral distribution function. This model is typical in that it gives an integrand with both pole and branch point singularities around which the contour must wend its way. We analyse the causes and nature of these singularities in Section 3.3. We are then ready to provide, in Section 3.4, a direct justification of our contour integral solution, showing that it does indeed satisfy the fundamental integral equation of Section 2.1.

### 3.1 Statement of the solution

Our contour integral solution is

$$f(E, J^2)=\frac{1}{4\pi^2\mathrm{i}\sqrt{2}}\frac{\partial}{\partial E}\int_0^{[\Psi_{\mathrm{env}}(E)+]}\frac{\mathrm{d}\Psi}{(\Psi-E)^{1/2}}\rho_1\left[\Psi, \frac{J^2}{2(\Psi-E)}\right]. \tag{3.1}$$

The integrand must be an analytic function of $\Psi$ on its contour of integration and in some adjacent region in the complex $\Psi$-plane for this contour integral to be meaningful. The density term in the integrand is obtained by replacing the $R^2$ in $\partial\rho(\Psi, R^2)/\partial\Psi$ by $J^2/2(\Psi-E)$. The subscript 1 denotes a partial derivative with respect to the first argument, a distinction which is necessary now that $\rho$ has $\Psi$-dependence through both of its arguments. The notation used here and subsequently in the upper limit is that of Whittaker & Watson (1927, section 12.22), and indicates that the contour is a loop which starts on the lower side of the real $\Psi$-axis at $\Psi=0$, the potential at large distances. The contour encircles $\Psi_{\rm env}(E)$ positively and ends at $\Psi=0$ on the upper side of the real $\Psi$-axis, as illustrated in Fig. 4(b). The contour crosses the real $\Psi$-axis to the right of $\Psi=E$ through a window $\mathscr{P}$, a window which represents the range of $\Psi$ values for which the arguments of the density in the integral (3.1) correspond to physically achieved values, i.e. for which the point $[\Psi, R^2=J^2/2)\Psi-E)]$ lies in the domain $\boldsymbol{P}$ of the physical density. Possible $\Psi$ and $R^2$ values are those for which the integration triangle of Fig. 1(a) lies within the envelope $\mathscr{E}$. Hence the window $\mathscr{P}$ is the interval $[\Psi_{\rm min}(E, J^2), \Psi_{\rm max}(E, J^2)]$ which we identified in Section 2.2, while the point $\Psi_{\rm env}(E)$ is simply a convenient choice of a point that is known always to lie within this window.

The contour generally encloses one or more cuts that lie along the real $\Psi$-axis. A cut is needed to define the fractional power $(\Psi-E)^{-1/2}$ in the integrand (3.1), unless this power is cancelled by some other term. Other cuts are needed when the density term $\rho_1[\Psi, J^2/2(\Psi-E)]$ has other branch points. All branch cuts must be placed in such a way that the density has its true physical value in the physically relevant window $\mathscr{P}$. The cuts must therefore avoid $\mathscr{P}$ as well as allowing the integrand of integral (3.1) to be an analytic function of $\Psi$ on its contour of integration. Thus it is convenient to place the cuts, which must emanate from branch points such as $E$ which are enclosed by the contour, along the real $\Psi$-axis, as in Figs 4(b) and 5(b).

### 3.1.1 *Eddington's (1916) spherical solution*

This is obtained by setting $J^2=0$ in equation (3.1). The integrand simplifies, although, unlike Eddington, we now have to assume that the function $\rho_1(\Psi, 0)=\partial\rho(\Psi, 0)/\partial\Psi$ is an analytic function of $\Psi$ for $\Psi$ real and on (0, 1]. The contour also simplifies to $\int_0^{(E+)}$, that is to a loop around the branch point at $\Psi=E$ and a cut along the real $\Psi$-axis to its left. The power $(\Psi-E)^{-1/2}$ is real and positive on the real $\Psi$-axis to the right of $E$ but has imaginary values of opposite sign along the two sides of the cut. We can convert the integral back to a real line integral by wrapping the path tightly around this cut from $O$ to $E$ to get the familiar form

$$f(E, 0)=\frac{1}{2\pi^2\sqrt{2}}\frac{\partial}{\partial E}\int_0^E\frac{{\rm d}\Psi}{(E-\Psi)^{1/2}}\frac{\partial\rho(\Psi, 0)}{\partial\Psi} \tag{3.2}$$

(Binney & Tremaine 1987, equation 4.140a). As well as being the full solution for the isotropic spherical case, equation (3.2) is now the solution for $f$ on the $J^2=0$ boundary of the domain $\boldsymbol{F}$.

### 3.1.2 *Alternative forms*

There are two useful alternative forms of the solution (3.1). Both are obtained by integration by parts, differentiation and by using the fact that the density vanishes at large distances where $\Psi=0$. One alternative form is

$$f(E, J^2)=\frac{1}{4\pi^2{\rm i}\sqrt{2}}\frac{\partial^2}{\partial E^2}\int_0^{[\Psi_{\rm env}(E)+]}\frac{{\rm d}\Psi}{(\Psi-E)^{1/2}}\rho\left[\Psi, \frac{J^2}{2(\Psi-E)}\right], \tag{3.3}$$

which has the simplest form of the integrand. We use it to locate and classify the singularities, because differentiation of the analytic $\rho$ does not introduce any new singularity or change the basic type of any existing singularity. The other alternative form is

$$f(E, J^2)=\frac{1}{4\pi^2{\rm i}\sqrt{2}}\int_0^{[\Psi_{\rm env}(E)+]}\frac{{\rm d}\Psi}{(\Psi-E)^{1/2}}\rho_{11}\left[\Psi, \frac{J^2}{2(\Psi-E)}\right], \tag{3.4}$$

in which the differentiation outside the integral has been carried out explicitly. This is a generalization of another formula given by Eddington (also Binney & Tremaine 1987, equation 4.140b), and is one possible form that might be used for the actual computation of a distribution function by numerical quadrature. The expression for the second derivative $\rho_{11}$ may be algebraically complicated, which is why we do not quote it for our examples, but its derivation is routine and can nowadays be delegated to a computer. Other computationally useful formulae for distribution functions may be obtained by first introducing a parametrization of the path into either of the integrals (3.1) or (3.3), and then differentiating the resulting integrand with respect to $E$.

## 3.2 The Kuzmin–Kutuzov (1962) model

This is a Stäckel model, although that feature plays no role here. Its potential is

$$\Psi(R^2, z^2)=\frac{1}{(a^2+c^2+R^2+z^2+2\sqrt{a^2c^2+c^2R^2+a^2z^2})^{1/2}}. \tag{3.5}$$

The two non-negative length parameters $a$ and $c$ are constrained by the condition

$$a+c=1, \tag{3.6}$$

because of our choice (equation 2.3) of units. The potential in the equatorial plane, which is

$$\Psi(R^2,0)=\frac{1}{c+\sqrt{a^2+R^2}}, \tag{3.7}$$

leads via equations (2.4) to the parametric representation

$$E=\frac{1}{2\sqrt{a^2+R^2}}\left[1+\frac{a^2-c^2}{(c+\sqrt{a^2+R^2})^2}\right], \qquad J^2=\frac{R^4}{\sqrt{a^2+R^2}(c+\sqrt{a^2+R^2})^2}, \tag{3.8}$$

for the boundary envelope $\mathscr{E}$ of the domain $\boldsymbol{F}$ in $(E, J^2)$-space.

Equation (3.5) for the potential also yields the relation

$$a^2+\sqrt{a^2c^2+c^2R^2+a^2z^2}=\frac{a}{\Psi}\sqrt{1-AR^2\Psi^2}. \tag{3.9}$$

This relation is needed for the elimination of $z^2$ from the expression for the density given by Dejonghe & de Zeeuw (1988, equation 4.10), and to derive the required formula

$$\rho(\Psi,R^2)=\frac{Mc^2\Psi^4}{4\pi a}\,\frac{(2-AR^2\Psi^2-a\Psi\sqrt{1-AR^2\Psi^2})}{(\sqrt{1-AR^2\Psi^2}-a\Psi)^3}. \tag{3.10}$$

Here, $A$ is the dimensionless ratio

$$A=\frac{a^2-c^2}{a^2}, \tag{3.11}$$

and provides a shape parameter for this one-parameter family of models. It either lies in the range $(0, 1)$ for an oblate model with $c<a$, or is negative for a prolate model with $a<c$. Fig. 3(a) displays $\rho(\Psi, R^2)$ for the $A=0.75$, $c/a=0.5$, oblate case. The dashed locus of points is where $\sqrt{1-AR^2\Psi^2}=a\Psi$ and $\rho$ is infinite. This curve lies outside the domain $\boldsymbol{P}$, but stops the density (3.10) having a Laplace transform with respect to $\Psi$.

The density in the integrand of equation (3.3) for $f$ is obtained from equation (3.10), after replacing $R^2$ with $J^2/2(\Psi-E)$, as

$$\rho\left[\Psi,\frac{J^2}{2(\Psi-E)}\right]=\frac{Mc^2\Psi^4}{4\pi a}\,\frac{\left\{2-\dfrac{AJ^2\Psi^2}{2(\Psi-E)}-a\Psi\left[1-\dfrac{AJ^2\Psi^2}{2(\Psi-E)}\right]^{1/2}\right\}}{\left\{\left[1-\dfrac{AJ^2\Psi^2}{2(\Psi-E)}\right]^{1/2}-a\Psi\right\}^3}. \tag{3.12}$$

Zeros of the denominator give pole singularities in the complex $\Psi$-plane, while zeros of the two square-root terms give two branch points, in addition to that at $E$, at

$$\left.\begin{matrix}\Psi_1\\ \Psi_2\end{matrix}\right\}=\frac{2E}{1\pm\sqrt{1-2AEJ^2}}. \tag{3.13}$$

Both branch points are real for any $(E, J^2)$-point of $\boldsymbol{F}$. Both are positive for an oblate model for which $0<A<1$ with $E<\Psi_1<2E$ and $2E<\Psi_2$. For a prolate model with $A<0$, $\Psi_2<0$ while $0<\Psi_1<E$. The different locations of the branch points require different cuts and evaluations of the square-root terms in $\rho$ for the two cases, which we discuss separately.

### 3.2.1 *Oblate case*

We can find where the real branch points and poles occur by studying, respectively, where the graph of $AJ^2\Psi^2/2(\Psi-E)$ equals 1, and where it intersects the parabola $1-a^2\Psi^2$. Fig. 4(a) illustrates the situation for an oblate case. Here, $AJ^2\Psi^2/2(\Psi-E)$ is

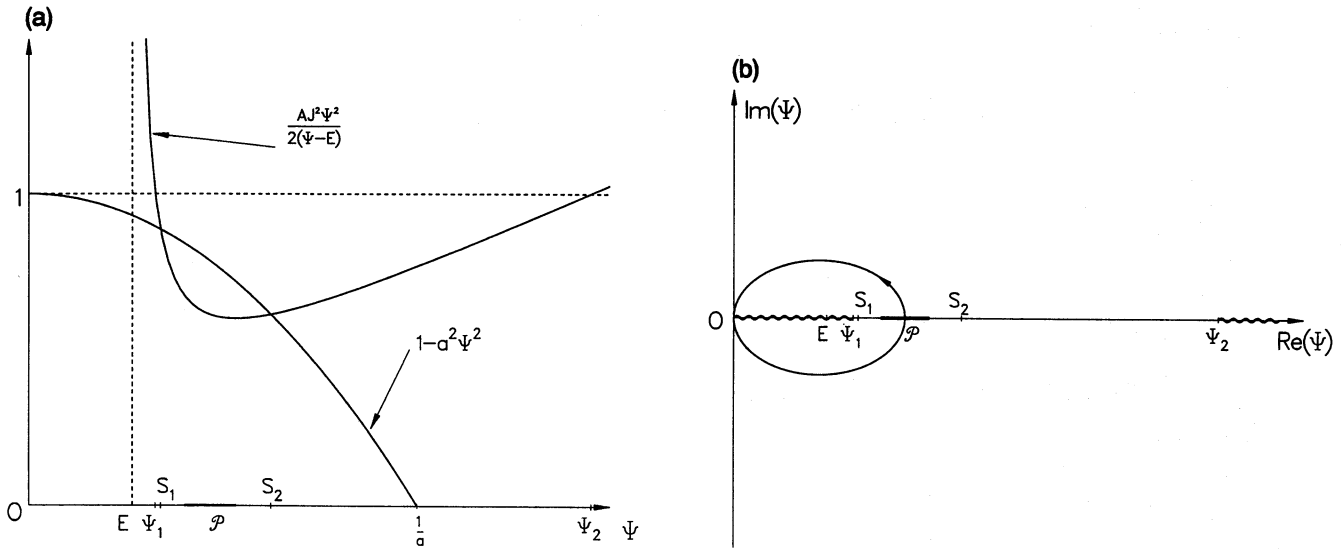


**Figure 4.** (a) Illustration for the geometrical analysis that locates the singularities, branch points $\Psi_1$ and $\Psi_2$ and poles $S_1$ and $S_2$, of the contour integral for an oblate ($A>0$) Kuzmin–Kutuzov density (3.12). The left-hand end of the physically realized window $\mathscr{P}$ must lie to the left of the minimum of $AJ^2\Psi^2/2(\Psi-E)$ at $\Psi=2E$, though this minimum need not lie in $\mathscr{P}$. (b) The looped contour of integration (with arrow) in the complex $\Psi$-plane for obtaining $f$ for an oblate $A>0$ case of the density (3.12). Cuts are denoted by wavy lines, and singularities (all on the real axis) are marked.

positive and less than 1 in the interval $(\Psi_1, \Psi_2)$, whose two ends correspond to zeros of $(1-AR^2\Psi^2)$. Equation (3.9) shows that these ends occur at unphysical complex values of the spatial $R^2$ and $z^2$ coordinates. The physically realized window $\mathscr{P}$, in which $(\sqrt{1-AR^2\Psi^2}-a\Psi)$ is positive and which we know must exist for any $(E, J^2)$ of $\boldsymbol{F}$, lies within the interval $(\Psi_1, \Psi_2)$. By continuity, there must also be zeros of $(\sqrt{1-AR^2\Psi^2}-a\Psi)$ sandwiched between the branch points and the two ends of the window $\mathscr{P}$. These are the pole singularities $S_1$ and $S_2$ at which the denominator of equation (3.12) vanishes and the density is infinite. These poles also correspond to unphysical complex values of the spatial coordinates by equation (3.9), and lie outside the physically relevant domain $\boldsymbol{P}$. To obtain the correct density in $\mathscr{P}$, we introduce two cuts along the real $\Psi$-axis, one to the right of $\Psi=\Psi_2$ and another to the left of $\Psi=\Psi_1$, and evaluate

$$\left[1-\frac{AJ^2\Psi^2}{2(\Psi-E)}\right]^{1/2}=\sqrt{\tfrac{1}{2}AJ^2}\,\frac{(\Psi_2-\Psi)^{1/2}(\Psi-\Psi_1)^{1/2}}{(\Psi-E)^{1/2}}, \tag{3.14}$$

with each half-power real for $\Psi$ real and $\Psi_1<\Psi<\Psi_2$. Now that this evaluation has been prescribed, we can show that there are no zeros of the denominator of equation (3.12) other than $S_1$ and $S_2$. The cubic in $\Psi$ that is obtained from squaring (3.14) and setting it equal to $a^2\Psi^2$ has a third negative root, not shown in Fig. 4(a), where the parabola $1-a^2\Psi^2$ intersects the other branch of $AJ^2\Psi^2/2(\Psi-E)$. Because it is negative and occurs where both the square root (3.14) and $-a\Psi$ are positive, it is not a zero of the denominator.

The contour for the oblate case is shown in Fig. 4(b). It encloses the branch points $E$ and $\Psi_1$ and the pole $S_1$, but no other singularities. The contour integral solution is specified now that the path of integration and the evaluation of fractional powers, and hence the integrand, have been prescribed. We have checked that it gives numerical values that agree with the quite different real integral solution (4.28a) of Dejonghe & de Zeeuw (1988), after correcting the following two misprints in the latter. The $(1-x_\epsilon^2)$ term in its numerator should be $(1-x_\epsilon)$, and the sign of the denominator term with the $2aE$ factor should be $-$, not $+$. For reasons given in Section B.2.2, we believe that there is no direct analytical transformation between the two different integrals for $f$.

### 3.2.2 *Prolate case*

The relevant curves, their intersections, and the locations of the singularities for this $A<0$ case are plotted in Fig. 5(a). We introduce cuts along the real $\Psi$-axis to the left of the branch points $\Psi_1$ and $\Psi_2$ which both lie to the left of $E$. The square-root terms in the density should now be evaluated as

$$\left[1-\frac{AJ^2\Psi^2}{2(\Psi-E)}\right]^{1/2}=\sqrt{-\tfrac{1}{2}AJ^2}\,\frac{(\Psi-\Psi_1)^{1/2}(\Psi-\Psi_2)^{1/2}}{(\Psi-E)^{1/2}}, \tag{3.15}$$

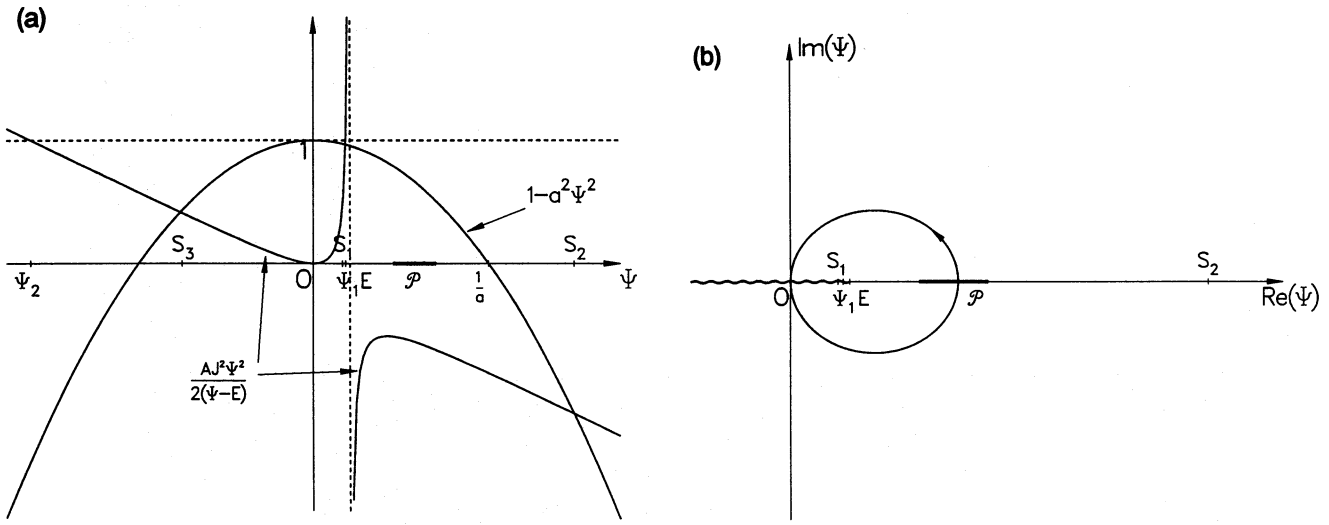


**Figure 5.** Same as Fig. 4, but for a prolate $A<0$ model. The physically realized segment $\mathscr{P}$ now lies also to the left of $\Psi = 1/a > 1$.

with each half-power real when $\Psi$ is real and greater than $E$. The square-root term (3.15) is now real on the whole of the real $\Psi$-axis to the right of $\Psi_1$. There is a pole singularity $S_1$ between $O$ and $\Psi_1$, and another $S_2$ to the right of $\Psi = a^{-1}$, and hence to the right of the window $\mathscr{P}$. Both terms of the denominator are positive at the third intersection $S_3$ of the two curves at a negative value of $\Psi$ between $\Psi_2$ and $O$, so that it is not a singularity. Because there are now no singularities between $E$ and the window $\mathscr{P}$, the contour needs only to enclose the segment of the real $\Psi$-axis between $O$ and $E$ on which $\Psi_1$ and $S_1$ lie, as shown in Fig. 5(b). With this contour and the evaluation specified in equation (3.15), we again obtain values of the distribution function $f$ which match those obtained from the corrected version of Dejonghe & de Zeeuw's integral (4.28a).

### 3.3 Types of singularity and their treatment

Branch points and poles of the function $\rho[\Psi, J^2/2(\Psi - E)]$ similar to those of the preceding example are the only kinds of singularity that we have encountered in the applications of our method that we have worked so far, as well as in all the examples that we present in this paper. The poles are all related to infinities of the density, which occur outside the physical domain $\boldsymbol{P}$. The branch points, other than at $\Psi = E$, are all associated with zeros of the Jacobian of the transformation from the $(\Psi, R^2)$ variables that we use to the spatial coordinates $(R^2, z^2)$, and hence with branch points of this transformation. The Jacobian is equal to $|\partial\Psi(R^2, z^2)/\partial z^2|$. It can vanish only outside the domain $\boldsymbol{P}$, because of the restriction that we imposed in Section 2 that $\Psi$ decrease with increasing $z^2$ in physical space. The simple density of the example in Lynden-Bell (1962) shows that it is possible for the contributions from such branch points to cancel from the density, but such cancellation is exceptional.

The non-physical nature of singularities in no way diminishes their significance for the evaluation of the distribution function via the contour integral formula. Mathematically, they occur at the roots of an equation of the form

$$U(\Psi, R^2\Psi) = 0, \tag{3.16}$$

where $U(\Psi, R^2\Psi)$ is some analytic component of the expression for the density $\rho(\Psi, R^2)$, such as either $1 - AR^2\Psi^2$ or $\sqrt{1 - AR^2\Psi^2} - a\Psi$ for the Kuzmin–Kutuzov density (3.10). The function $U(\Psi, R^2\Psi)$ is real and positive when its arguments lie in $\boldsymbol{P}^*$. Also, equation (3.16) has a unique real solution,

$$R^2\Psi = u(\Psi), \tag{3.17}$$

for $R^2\Psi$ in terms of $\Psi$. The roots of equation (3.16) cause the integrand of our contour integral to be singular at points in the complex $\Psi$-plane at which

$$U\left[\Psi, \frac{J^2\Psi}{2(\Psi - E)}\right] = 0. \tag{3.18}$$

These singularities can be grouped into two types according to their behaviour as the $J^2 = 0$ boundary of domain $\boldsymbol{F}$ is approached. We label as type I those singularities for which $\Psi \to E$ as $J^2 \to 0$. They are enclosed within the contour of integration

for $J^2$ small. Their generic behaviour is as

$$\Psi = E + \frac{J^2}{2\beta(E)} + o(J^2), \tag{3.19}$$

where $\beta(E)$ is a root of the equation

$$U[E, E\beta(E)] = 0. \tag{3.20}$$

The positivity of $U$ throughout the domain $\boldsymbol{P}^*$, as shown in Fig. 3(b), shows that

$$\lim_{E\to 0} E\beta(E) = \infty.$$

Both the $\Psi_1$ and $S_1$ singularities of the Kuzmin–Kutuzov model are of this type I; so too are any singularities that appear on the real $\Psi$-axis in the gap which opens up for $J^2 = 0+$ between $E$ and the window $\mathscr{P}$. Type I singularities are real because of the real solution (3.17) of equation (3.16). They may have negative $\beta(E)$ and lie to the left of $E$, as the case of the prolate Kuzmin–Kutuzov model shows. The example of Appendix D shows that a type I singularity may move through the origin and thus out of the integration contour, thereby causing an abrupt change in the distribution function.

We define type II singularities as those that tend to some root $\Psi_0$ of the equation $U(\Psi, 0) = 0$ in the $J^2 \to 0$ limit. Their generic behaviour is as

$$\Psi = \Psi_0 - \frac{J^2\Psi_0 U_2(\Psi_0, 0)}{2(\Psi_0 - E)\, U_1(\Psi_0, 0)} + o(J^2), \tag{3.21}$$

where the subscripts on $U$ again denote partial derivatives. Type II singularities may occur in complex conjugate pairs as in Satoh's model of Section 4.2. Real type II singularities cannot lie in the $0 \le \Psi \le 1$ range, because this would cause the arguments of $U$ to lie in $\boldsymbol{P}^*$. They therefore lie outside the contour of integration. The $\Psi = \Psi_2$ branch point of the Kuzmin–Kutuzov model, for which $\Psi_2 \sim 2/(AJ^2)$ as $J^2 \to 0$, is an exceptional type II case which is associated with an infinite root of the equation $U(\Psi, 0) = 0$ and to which equation (3.21) does not apply.

### 3.4 Justification of the contour integral solution

We use the first derivative version (3.1) of our solution and substitute it into the second form of the right-hand side of equation (2.1), in which the $E$-integration is innermost. The inner integration can then be done explicitly. The result, when a dummy variable $\Phi$ of integration is used in the contour integral, is

$$\frac{2\pi}{R}\int_0^{2R^2\Psi}\frac{\mathrm{d}J^2}{\sqrt{J^2}}\int_0^{\Psi-(J^2/2R^2)} f(E, J^2)\,\mathrm{d}E = \frac{1}{2\pi\mathrm{i}R}\int_0^{2R^2\Psi}\frac{\mathrm{d}J^2}{\sqrt{J^2}}\int_0^{[\Psi_{\mathrm{env}}[\Psi-(J^2/2R^2)]+}\frac{\mathrm{d}\Phi}{[2(\Phi-\Psi)+J^2/R^2]^{1/2}}\,\rho_1\left[\Phi, \frac{J^2}{2(\Phi-\Psi)+J^2/R^2}\right], \tag{3.22}$$

provided that

$$\lim_{E\to 0}\int_0^{[\Psi_{\mathrm{env}}(E)+]}\frac{\mathrm{d}\Phi}{(\Phi-E)^{1/2}}\,\rho_1\left[\Phi, \frac{J^2}{2(\Phi-E)}\right] = 0. \tag{3.23}$$

The contour can be shrunk to a small contour as $E \to 0$ because it crosses the real $\Psi$-axis at $\Psi_{\mathrm{env}}(E) \sim 2E$. The condition (3.23) is then satisfied, provided that the density tends to zero sufficiently rapidly at large distances where $\Psi \to 0$. It is well satisfied by all the densities of our examples.

The next step is to simplify the right-hand side of equation (3.22) by changing the outer variable of integration from $J^2$ to $B = \Psi - (J^2/2R^2)$, so that it becomes

$$\frac{1}{2\pi\mathrm{i}}\int_0^{\Psi}\frac{\mathrm{d}B}{(\Psi-B)^{1/2}}\int_0^{[\Psi_{\mathrm{env}}(B)+]}\frac{\mathrm{d}\Phi}{(\Phi-B)^{1/2}}\,\rho_1\left[\Phi, \frac{R^2(\Psi-B)}{\Phi-B}\right]. \tag{3.24}$$

It is now evident that the point $\Phi = \Psi$ lies in the physically relevant window $\mathscr{P}$ through which the contour of the inner integral must cross the real $\Phi$-axis, because the arguments of $\rho_1$ are $(\Psi, R^2)$ there. We can therefore rewrite the inner $\int_0^{[\Psi_{\mathrm{env}}(B)+]}$ integration as an $\int_0^{(\Psi+)}$ integration which is independent of $B$. This independence is necessary to allow us to interchange the order of the integrations to obtain

$$\frac{1}{2\pi\mathrm{i}}\int_0^{(\Psi+)}\mathrm{d}\Phi\int_0^{\Psi}\frac{\mathrm{d}B}{(\Psi-B)^{1/2}(\Phi-B)^{1/2}}\,\rho_1\left[\Phi, \frac{R^2(\Psi-B)}{\Phi-B}\right]. \tag{3.25}$$

We then change the inner variable of integration from $B$ to

$$\zeta = \Phi\left(\frac{\Psi - B}{\Phi - B}\right). \tag{3.26}$$

This simplifies the integral (3.25) to

$$\frac{1}{2\pi i}\int_0^{(\Psi+)} d\Phi \int_0^{\Psi} \frac{d\zeta}{(\Phi-\zeta)}\left(\frac{\Phi}{\zeta}\right)^{1/2} \rho_1\left(\Phi, \frac{R^2\zeta}{\Phi}\right), \tag{3.27}$$

but also changes the inner path of integration, because the change of variables (3.26) is a complex one now that the outer variable of integration $\Phi$ lies on the complex contour looping around $\Psi$. Specifically, the inner $\zeta$-integration is along a path that is the image, under the mapping (3.26), of the real $B$-axis from $O$ to $\Psi$. This image is a circular arc because the mapping is bilinear. In particular, it is the segment from $O$ and $\Psi$, but not containing $\Phi$, of the circle defined by the three points $O$, $\Psi$ and $\Phi$, which are the images of the three points $\Psi$, $O$ and $\infty$ on the real $B$-axis (see Fig. 6). We now wish to change the path of $\zeta$-integration from this circular arc to the real $\zeta$-axis, which we can do provided that there are no singularities of the integrand lying within the region, shaded in Fig. 6, between the arc and the real axis. The $O(\zeta^{-1/2})$ behaviour of the integrand near $\zeta = 0$ means that the path can be modified in its neighbourhood. The simple pole singularity at $\zeta = \Phi$ lies outside the shaded region on the opposite side of the real $\zeta$-axis. We must also, however, consider the singularities of the integrand that arise from the $\rho_1(\Phi, R^2\zeta/\Phi)$ component, which we must now regard as a function of $\zeta$.

We can analyse the singularities that are contributed by the $\rho_1$ component for each individual model. The Kuzmin–Kutuzov model, for instance, has a branch point at $\zeta = 1/(AR^2\Phi)$ and a pole at $\zeta = 1/(AR^2\Phi) + a^2\Phi/(AR^2)$. The branch point evidently lies outside the shaded region for the $A<0$ prolate case (see Fig. 6), but the oblate $A>0$ case requires a more careful analysis. However, a generally applicable discussion is clearly preferable, and we shall now give one that applies to all the examples discussed in this paper. We restrict the range of the outer variable of integration $\Phi$ by wrapping its path of integration tightly around the segment of the real $\Phi$-axis between $O$ and $\Psi$. This restricts $\Phi$ to have a small imaginary part and a real part which is in or close to the interval $[0, \Psi]$. We then make use of the fact, noted in Section 3.3, that the singularities of the $\rho_1$ component are all associated with values of $\zeta$ for which equations of the form

$$U(\Phi, R^2\zeta) = 0, \qquad R^2\zeta = u(\Phi) \tag{3.28}$$

are satisfied with $u$ real when $\Phi$ is real. The imaginary part of $\zeta$ is therefore also small. The function $U$ is analytic and positive not only at a point $(\Psi, R^2\Psi)$ of $\boldsymbol{P}^*$, but also throughout the rectangle $\boldsymbol{R}$ of points of $\boldsymbol{P}^*$, for which $(\Psi, R^2\Psi)$ is the upper right corner (see Fig. 3b). Hence there is an open set $\boldsymbol{R}^+$ of $\boldsymbol{C}^2$, the space of two complex variables, containing $\boldsymbol{R}$ in which $U$ is also analytic and its real part positive. Any singularity $(\Phi, R^2\zeta)$ for which equation (3.28) is satisfied must lie outside $\boldsymbol{R}^+$, so that Re $\zeta$ must lie outside the interval $[0, \Psi]$. Hence singularities contributed by the $\rho_1$ component lie outside the region enclosed between

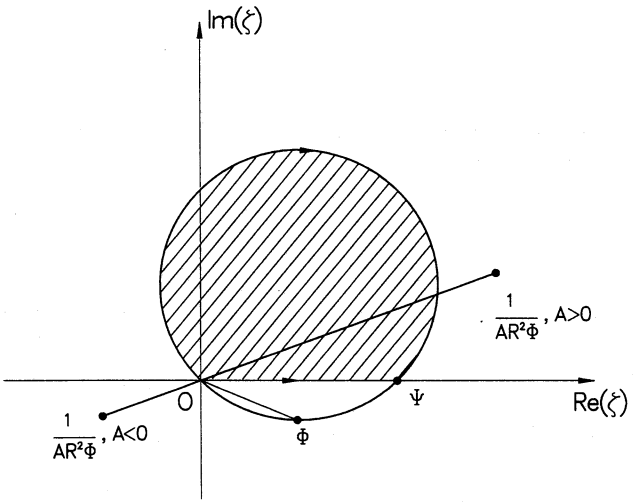


**Figure 6.** The $\zeta$-plane, where $\zeta$ is the variable defined by equation (3.26). The point $\Phi$ has a small imaginary part which is exaggerated in the figure. We argue that the path of integration for the inner integral of (3.27) can be changed from the part of the circle above the real $\zeta$-axis to the real $\zeta$-axis. This requires that no singularities of the integrand lie in the shaded region between the two paths. $1/AR^2\Phi$ is such a singularity of the Kuzmin–Kutuzov model, and lies outside the shaded region because its real part exceeds $\Psi$ when $A$ is positive, and is negative when $A$ is negative.

the two $\zeta$-paths of integration, as in the example illustrated in Fig. 6. The $\zeta$-path of integration can therefore be changed to lie along the real axis, and we can henceforth treat $\zeta$ as a real variable. (Cuts associated with branch points must also be such as to avoid $\boldsymbol{R}^+$.)

Now that $\zeta$ is real, we interchange orders of integration again. The $\Phi$-integration can be performed as an elementary application of Cauchy's Residue Theorem. The only singularity of the integrand as a function of $\Phi$ is the simple pole at $\Phi=\zeta$. It lies on the real $\Phi$-axis within the contour. There are no other enclosed singularities because $\rho_1$ is analytic in $\boldsymbol{R}^+$. Hence the integral (3.27) can be evaluated as

$$\frac{1}{2\pi \mathrm{i}}\int_0^{\Psi} \mathrm{d}\zeta \int_0^{(\Psi+)} \frac{\mathrm{d}\Phi}{(\Phi-\zeta)}\left(\frac{\Phi}{\zeta}\right)^{1/2}\rho_1\left[\Phi, \frac{R^2\zeta}{\Phi}\right]=\int_0^{\Psi}\rho_1(\zeta, R^2)\,\mathrm{d}\zeta=\rho(\Psi, R^2). \tag{3.29}$$

The final step in equation (3.29) is an elementary real integration with respect to $\zeta$. It completes a rigorous justification of our contour integral formula for densities that are analytic, and whose singularities satisfy the conditions imposed in Section 3.3.

## 4 TWO NEW DISTRIBUTION FUNCTIONS

This section contains two further applications of our contour integral solution. In Section 4.1 we compute distribution functions for the family of flattened isochrones studied by Evans et al. (1990). These models can, in fact, be prolate and stretched, as well as flattened and oblate. Evans et al. calculated their thin orbit distribution functions, but gave a two-integral distribution function only for the most flattened ($c=0$) model, as a doubly infinite series of hypergeometric functions. In Section 4.2 we compute distribution functions for a family of oblate models due to Satoh (1980), and used by him to model NGC 4697. He solved stellar hydrodynamic equations but gave no distribution function.

### 4.1 The 'flattened' isochrone

These models have the gravitational potential

$$\Psi(R^2, z^2)=\frac{(X+aY+c^2)}{Y(X+aY+a^2)}, \tag{4.1}$$

where $a$ and $c$ are two non-negative length-scales, and $X$ and $Y$ are the quantities

$$X=\sqrt{a^2c^2+c^2R^2+a^2z^2}, \qquad Y=\sqrt{a^2+c^2+R^2+z^2+2X}. \tag{4.2}$$

The gravitational potential in the equatorial plane $z=0$ is that of the isochrone

$$\Psi(R^2, 0)=\frac{1}{a+\sqrt{a^2+R^2}}. \tag{4.3}$$

The length-scale $a$ has the fixed value 0.5 in the units defined in equation (2.3), but we shall retain it symbolically in our working. The parametric representation for the envelope $\mathscr{E}$ is

$$E=\frac{1}{2\sqrt{a^2+R^2}}, \qquad J^2=\frac{(\sqrt{a^2+R^2}-a)^2}{\sqrt{a^2+R^2}}. \tag{4.4}$$

Exceptionally, the parameter $R^2$ can be eliminated between these equations to give the explicit formula for $\mathscr{E}$ of

$$2EJ^2=(1-2aE)^2. \tag{4.5}$$

Explicit formulae can also be derived for the important points that the envelope defines and which are illustrated in Fig. 1(b). They are

$$\Psi_{\mathrm{env}}(E)=\frac{2E}{1+2aE}, \qquad \left.\begin{matrix}\Psi_{\mathrm{min}}(E, J^2)\\ \Psi_{\mathrm{max}}(E, J^2)\end{matrix}\right\}=\frac{2E}{(1+2aE)\pm\sqrt{(1-2aE)^2-2EJ^2}}. \tag{4.6}$$

Hence we have an explicit formula for the window $\mathscr{P}$, and do not have to locate it numerically as in other examples.

Evans et al. (1990) give the density as

$$\rho(\Psi, R^2)=\frac{M}{4\pi X^3 Y^3(X+aY+a^2)^2}[(2a^2-c^2)X^4+2a(2a^2-c^2)X^3Y+c^2(3a^2-c^2)X^2Y^2$$
$$+(2a^4+2a^2c^2-c^4)X^3+2ac^4XY(Y^2-X)+6a^3c^2X^2Y+a^2c^4Y^2(Y^2+3X) \tag{4.7}$$
$$+3a^4C^2X^2+2a^3c^4Y(Y^2+X)+a^4c^4(Y^2+X)],$$

where

$$X=\frac{a^2(1-2a\Psi-R^2\Psi^2)+a(a+R^2\Psi)\sqrt{1-A\Psi(2a+R^2\Psi)}}{\Psi(2a+R^2\Psi)}=\frac{a^2(A-1)(a+R^2\Psi)+a(a^2+R^2)\sqrt{1-A\Psi(2a+R^2\Psi)}}{a+R^2\Psi-a\sqrt{1-A\Psi(2a+R^2\Psi)}},$$

$$Y=\frac{a+R^2\Psi+a\sqrt{1-A\Psi(2a+R^2\Psi)}}{\Psi(2a+R^2\Psi)}=\frac{Aa^2+R^2}{a+R^2\Psi-a\sqrt{1-A\Psi(2a+R^2\Psi)}}, \tag{4.8}$$

$$X+aY+a^2=\frac{a}{\Psi}[1+\sqrt{1-A\Psi(2a+R^2\Psi)}].$$

Here $A$ is the same dimensionless ratio as that defined in equation (3.11) of Section 3.2, with the ranges (0, 1) for oblate models and $(-\infty, 0)$ for prolate ones. Both of the expressions for $X$ and $Y$ are needed.

Despite its apparently greater complexity, the singularity structure of this model is the same as that of the Kuzmin–Kutuzov model. The density $\rho[\Psi, J^2/2(\Psi-E)]$ has two extra branch points, given by the zeros of $1-A\Psi(2a+R^2\Psi)$ which lie outside $\boldsymbol{P}$, at

$$\left.\begin{matrix}\Psi_1(E, J^2)\\ \Psi_2(E, J^2)\end{matrix}\right\}=\frac{2E}{(1+2aAE)\pm\sqrt{(1-2aAE)^2-2AEJ^2}}. \tag{4.9}$$

Both are real and positive and straddle $\mathscr{P}$ in the oblate $A>0$ case, while one is in $(0, E)$ and the other negative in the prolate $A<0$ case. We place the cuts in the same way as in Figs 4(b) and 5(b).

For the oblate case which we discuss first, we evaluate the square-root components of $X$ and $Y$ as

$$\left\{1-A\Psi\left[2a+\frac{J^2\Psi}{2(\Psi-E)}\right]\right\}^{1/2}=\sqrt{\tfrac{1}{2}A(J^2+4a)}\,\frac{(\Psi_2-\Psi)^{1/2}(\Psi-\Psi_1)^{1/2}}{(\Psi-E)^{1/2}}. \tag{4.10}$$

Other singularities of our integrand could now arise from the density $\rho[\Psi, J^2/2(\Psi-E)]$ from any of five possible sources: poles of either $X$ or $Y$, and zeros of any of $Y$, $X+aY+a^2$, and $X$. The following discussion shows, after examining the other possibilities in turn, that they can arise only from zeros of $X$. Both $X$ and $Y$ do have simple poles at $\Psi=0$, where $X\sim a/\Psi$ and $Y\sim 1/\Psi$, but $\rho[\Psi, J^2/2(\Psi-E)]=O(\Psi^4)$ and is analytic here. The second expressions for $X$ and $Y$ in equations (4.8) show that neither is singular at the point $\Psi=4aE/(4a+J^2)$, corresponding to the zero of $(2a+R^2\Psi)$. This is an inconsequential removable singularity at which the first expressions for $X$ and $Y$ have 0/0 forms. There is no zero of $Y$ at $\Psi=E-J^2/2Aa^2$ associated with the zero of $R^2=-Aa^2$, which is another 0/0 form. $X+aY+a^2$ does not vanish, because the cuts do not allow the square root ever to be equal to $-1$. This leaves zeros of $X$ as the only remaining possibility. There are two zeros $S_1$ and $S_2$ of $X$, straddling $\mathscr{P}$ and in the gap between the two branch points $\Psi_1$ and $\Psi_2$. Their existence follows from the fact that the numerator of the first expression for $X$ in equations (4.8) is positive in $\mathscr{P}$, but negative at the branch points where it is $a^2(1-1/A)$, and hence has zeros in between. That there cannot be other roots is seen by analysing the polynomial obtained by setting the same numerator of $X$ to zero and squaring. This is now a quartic, but one of its roots is the removable singularity found earlier at $\Psi=4aE/(4a+J^2)$. The root remaining, apart from $S_1$ and $S_2$, is real, but it is not another zero of $X$. Once again, therefore, there are no singularities off the real axis in the complex plane. The path encloses $\Psi_1$ and $S_1$, both of which are type I singularities, but neither of the type II singularities $\Psi_2$ and $S_2$.

For the prolate $A<0$ case, we evaluate the square-root components of $X$ and $Y$ as

$$\left\{1-A\Psi\left[2a+\frac{J^2\Psi}{2(\Psi-E)}\right]\right\}^{1/2}=\sqrt{-\tfrac{1}{2}A(J^2+4a)}\,\frac{(\Psi-\Psi_1)^{1/2}(\Psi-\Psi_2)^{1/2}}{(\Psi-E)^{1/2}}. \tag{4.11}$$

The discussion already given for the oblate case, which shows that the only other singularities from the $\rho$ term arise from zeros of $X$, still applies. The integrand again has poles at two real zeros of $X$. One is at $S_2$, which lies to the right of $\mathscr{P}$ and is at $(2-A)/2a$

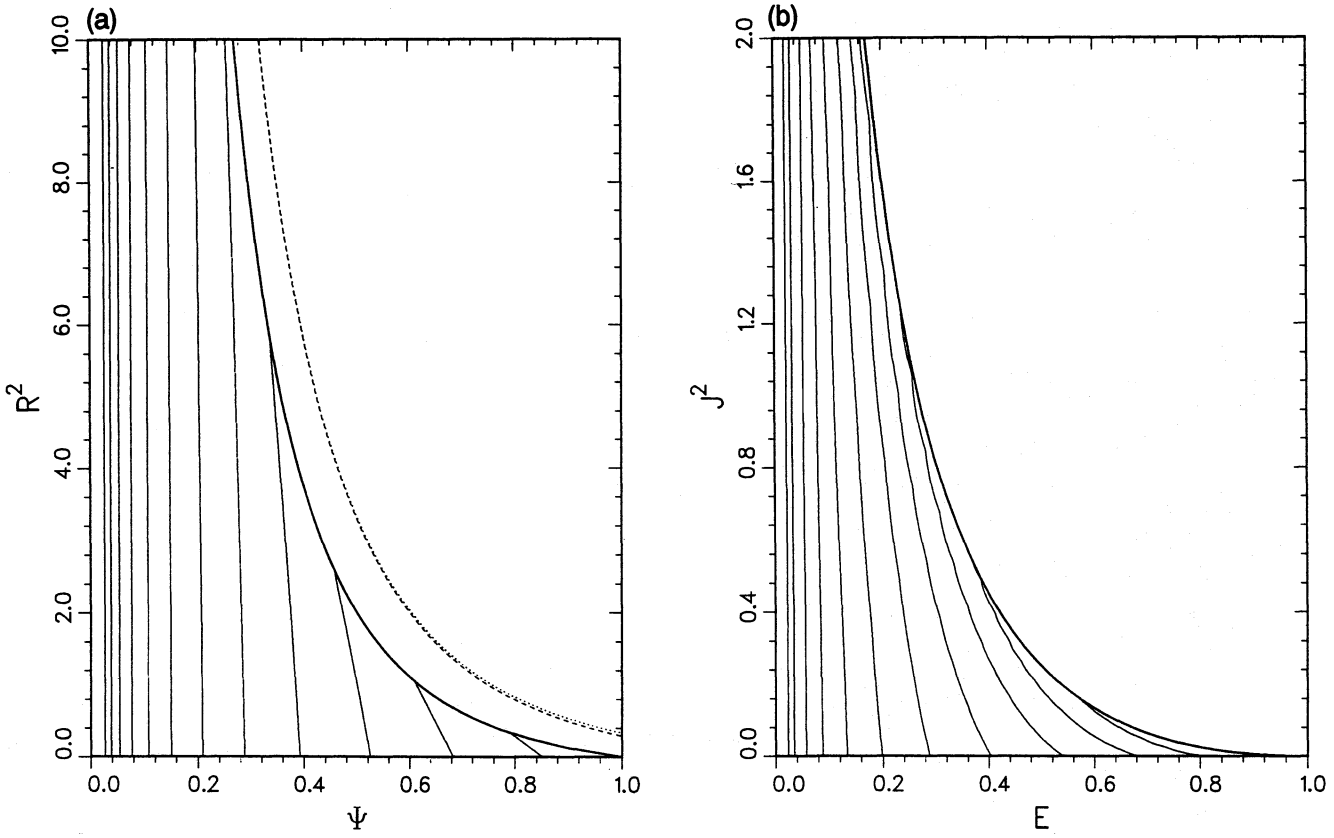


**Figure 7.** (a) The density $\rho(\Psi, R^2)$ and (b) the distribution function $f(E, J^2)$ for the oblate flattened isochrone with $c/a = 0.5$. Successive contour levels differ by factors of 0.25. The dashed and dotted curves have the same significance as in Fig. 3. Note that the domain $\boldsymbol{F}$ is narrower than the domain $\boldsymbol{P}$; their respective boundaries tend to $E \sim 1/2J^2$ and $\Psi \sim 1/R$ in the upper regions.

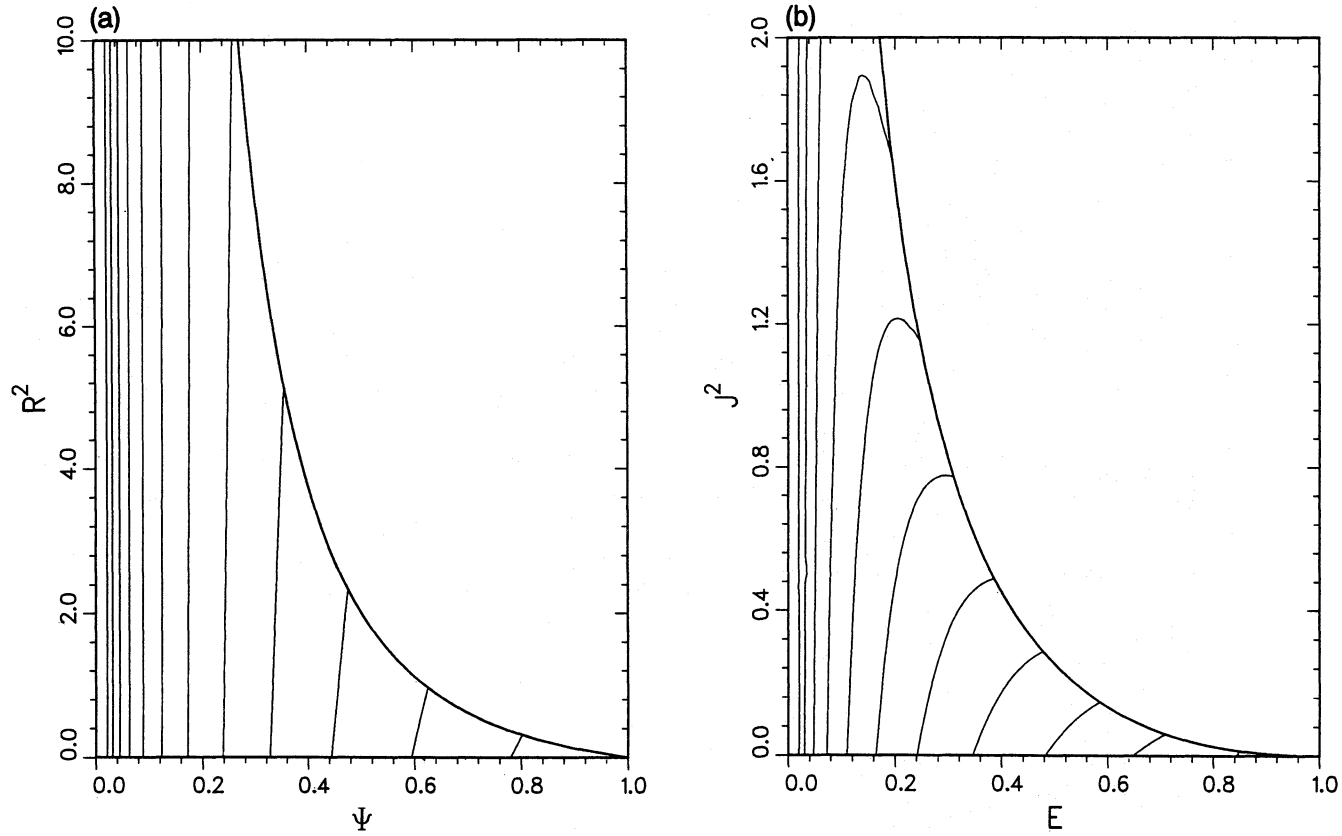


**Figure 8.** Same as Fig. 7 but for a prolate model with $c/a = 1.2$. There is a curve on which $\rho$ is infinite and which does not appear because it lies to the right of the region shown. It crosses the $\Psi$-axis at $\Psi = 2 - A > 1$, and then asymptotes to $\Psi = \infty$ at $R^2 = a^2/(-A)$.

in the $J^2 \to 0$ limit. It occurs because the numerator of the first expression for $X$ in equation (4.8) is positive in $\mathscr{P}$ but large and negative as $\Psi \to \infty$. The other zero is at $S_1$ in the $(0, \Psi_1)$ interval. The $X$ numerator is now positive at both ends of this interval, but changes sign at both $S_1$ and $\Psi = 4aE/(4a + J^2)$. As with the prolate Kuzmin–Kutuzov model, there are no other singularities, and the contour can be shrunk so that it encloses only the $[0, E]$ segment of the real $\Psi$-axis.

Densities and distribution functions for two of these models, one oblate and one prolate, are displayed in Figs 7 and 8. All quantities decrease from their peak values in the lower right-hand corner. The equidensity contours slope differently in the two cases because of their different orientations relative to the equipotentials (cf. Fig. 2 and its caption). Contours of $f$ reflect the trends of those of $\rho$ in exaggerated form. The density of Fig. 7(a) is qualitatively similar to that of the Kuzmin–Kutuzov model of Fig. 3(a), which has the same value of $c/a$. The two distribution functions are also qualitatively similar to those of Dejonghe & de Zeeuw's (1988) fig. 6. Negative values of $f$ develop on $\mathscr{E}$ for $c/a > 1.22$, which is the extreme two-integral prolate model in this case.

### 4.2 Satoh's $n = \infty$ model

The potential of this model (Satoh 1980) is

$$\Psi(R^2, z^2) = \frac{1}{[R^2 + z^2 + a(a + 2\sqrt{z^2 + b^2})]^{1/2}}, \tag{4.12}$$

where $a$ and $b$ are two positive length-scales which satisfy the relation

$$a(a + 2b) = 1, \tag{4.13}$$

because of the units introduced in equation (2.3), so that $a$ is restricted to the [0, 1] range, while $b = (a^{-1} - a)/2$ is unbounded. All of Satoh's models are oblate. The parametric equation for the envelope $\mathscr{E}$ is now

$$E = \frac{(1/2)R^2 + 1}{(R^2 + 1)^{3/2}}, \qquad J^2 = \frac{R^4}{(R^2 + 1)^{3/2}}, \tag{4.14}$$

and is the same for all cases.

The density can be found in terms of $R^2$ and $\Psi$ using the potential (4.12) and Satoh's equation (8) as

$$\rho(\Psi, R^2) = \frac{Mab^2\Psi^6}{4\pi} \frac{[7 - 6R^2\Psi^2 + 3(a^2 + 2b^2)\Psi^2 - 9a\Psi\sqrt{1 - R^2\Psi^2 + b^2\Psi^2}]}{[\sqrt{1 - R^2\Psi^2 + b^2\Psi^2} - a\Psi]^3}. \tag{4.15}$$

The singularities of the integrand that occur now, when $R^2$ is replaced by $J^2/2(\Psi - E)$ in $\rho(\Psi, R^2)$ as usual, all occur at roots of a single equation

$$1 - \frac{EJ^2\psi^2}{2(\psi - 1)} + \chi\psi^2 = 0, \qquad \Psi = E\psi. \tag{4.16}$$

This cubic in the scaled variable $\psi$ contains two parameters. The newly introduced parameter $\chi$ is $b^2E^2$ for the branch points given by zeros of the square roots, and $(b^2 - a^2)E^2$ for the poles given by zeros of the denominator. Fig. 9(b) shows the relevant domain of the two parameters $EJ^2$ and $\chi$. $EJ^2$ is limited to the range [0, 0.5], while $\chi$ can be unboundedly large for $\chi = b^2E^2$ because of the unboundedness of $b$. $\chi = (b^2 - a^2)E^2$ can be negative, but not less than $\chi = -E^2$ because $b^2 - a^2 \geq -1$. The lower boundary in Fig. 9(b) is the $(EJ^2, -E^2)$ curve corresponding to the envelope $\mathscr{E}$ of equation (4.14).

The different real positive roots of equation (4.16) can best be understood by reference to Fig. 9(a), in which they occur at intersections of the graphs of $EJ^2\psi^2/2(\psi - 1)$ and the parabola $1 + \chi\psi^2$. For an upward-bending parabola, there is always an intersection between $\psi = 1$ and the minimum of the other curve at $\psi = 2$. The parabola grows faster as $\psi \to \infty$, and there is another pair of intersections if $\chi$ is small enough and the parabola sufficiently flat that this more rapid growth is delayed until large $\chi$. If $\chi$ is too large for this to happen, the other two roots of equation (4.16) are a complex conjugate pair, as they are at $\psi = \pm i/\sqrt{\chi}$ in the $EJ^2 \to 0$ limit. The transition between these two cases occurs when equation (4.16) has a double root. This happens when both equation (4.16) and its derivative vanish, a pair of equations which can be solved to give the following parametric representation of the transition:

$$EJ^2 = \frac{4(\psi - 1)^2}{\psi^3}, \qquad \chi = \frac{\psi - 2}{\psi^3}. \tag{4.17}$$

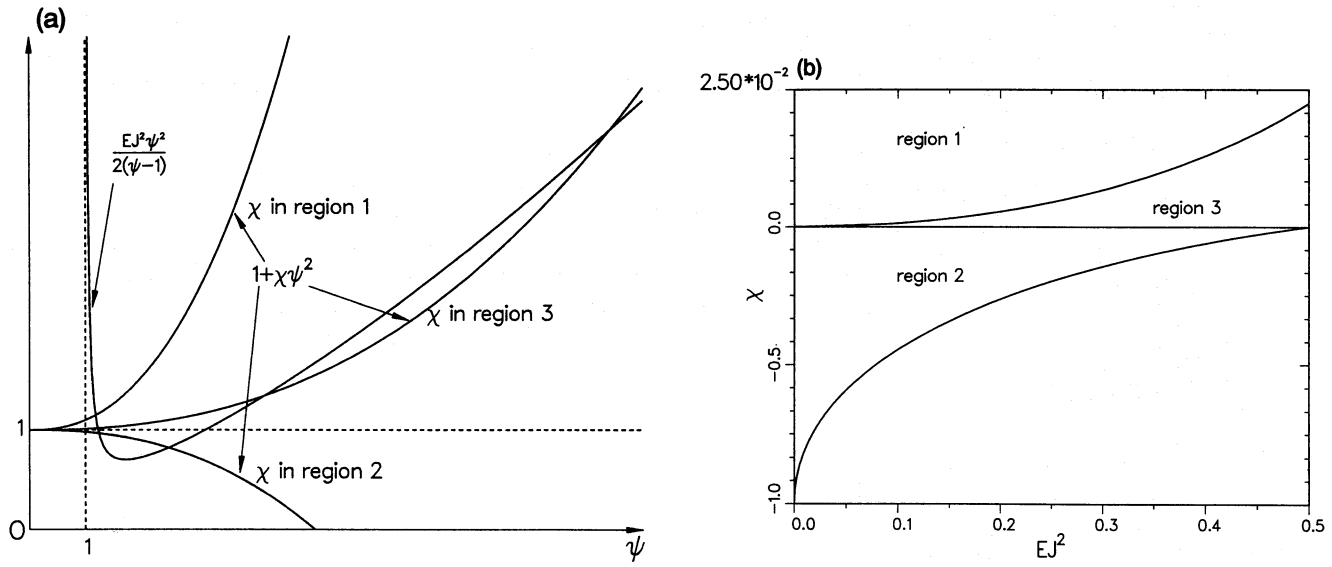


**Figure 9.** (a) Three cases of the intersection of the curve $EJ^2\psi^2/2(\psi-1)$ with the parabola $1+\chi\psi^2$ which locate real positive singularities for the contour integral of the Satoh model. (b) Regions of the $(EJ^2, \chi)$ parameter space in which the three cases of part (a) occur. Equation (4.16) has a complex conjugate pair of roots for parameters in region 1, which extends to large $\chi$. Note the different scales used on the two parts of the $\chi$-axis.

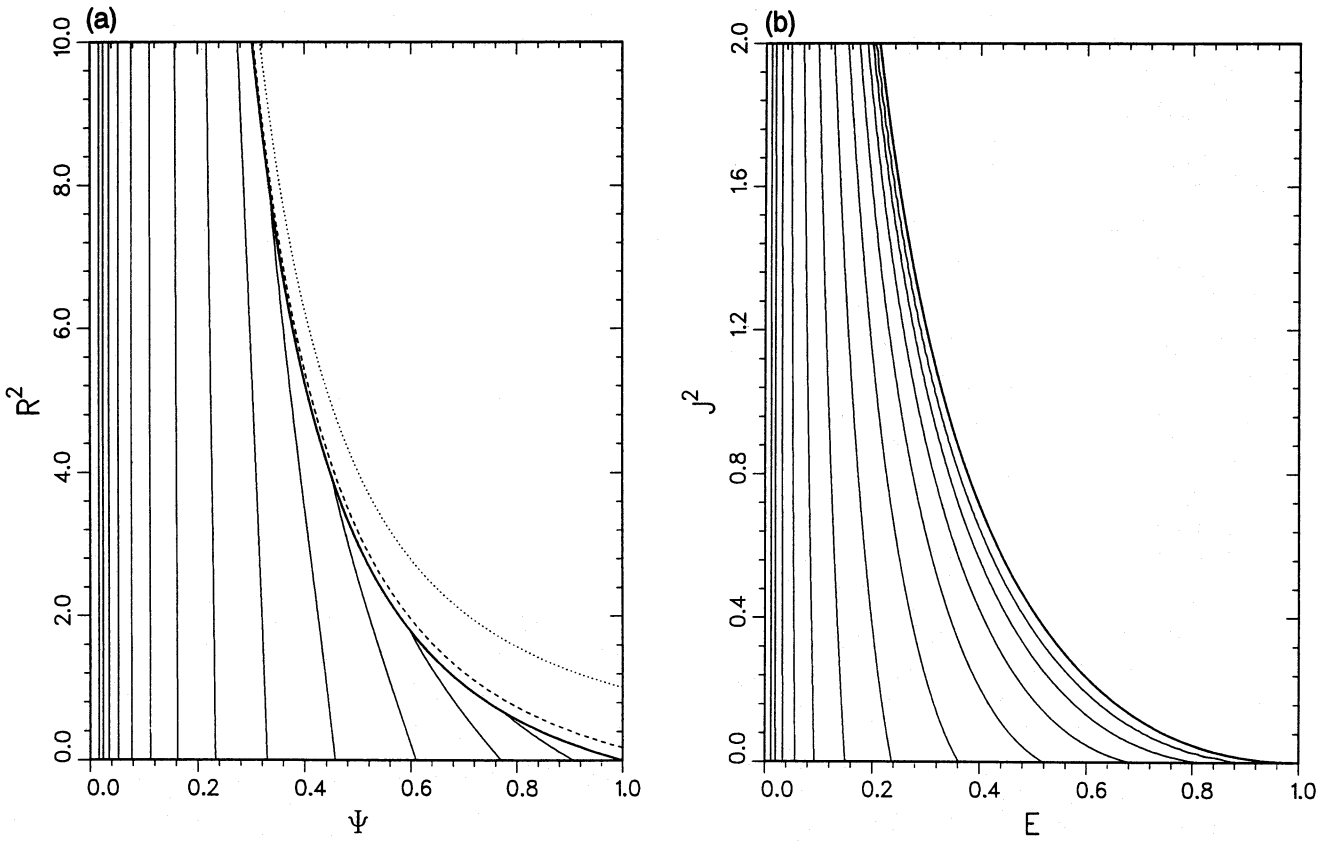


**Figure 10.** Same as Fig. 7 but for a Satoh model with $b/a = 0.1$. Successive contour levels here differ by factors of 0.1.

This is the boundary between the regions marked 1 and 3 in Fig. 9(b), and is given by equations (4.17) with values of $\psi$ in the range $[3+\sqrt{5}, \infty)$, for which $EJ^2 \leq 1/2$. For small negative $\chi$, the parabola bends down and there are two positive intersections. These merge and there is again a double root at the lower boundary in Fig. 9(b). This is another double-root transition, and is described by equations (4.17) with $\psi$ in the range [1, 2]. To verify that this boundary also corresponds to the values of $EJ^2$ and $\chi = -E^2$ for the envelope $\mathscr{E}$, substitute the value $\psi = 2(R^2+1)/(R^2+2)$ into equation (4.17) to reproduce equations (4.14).

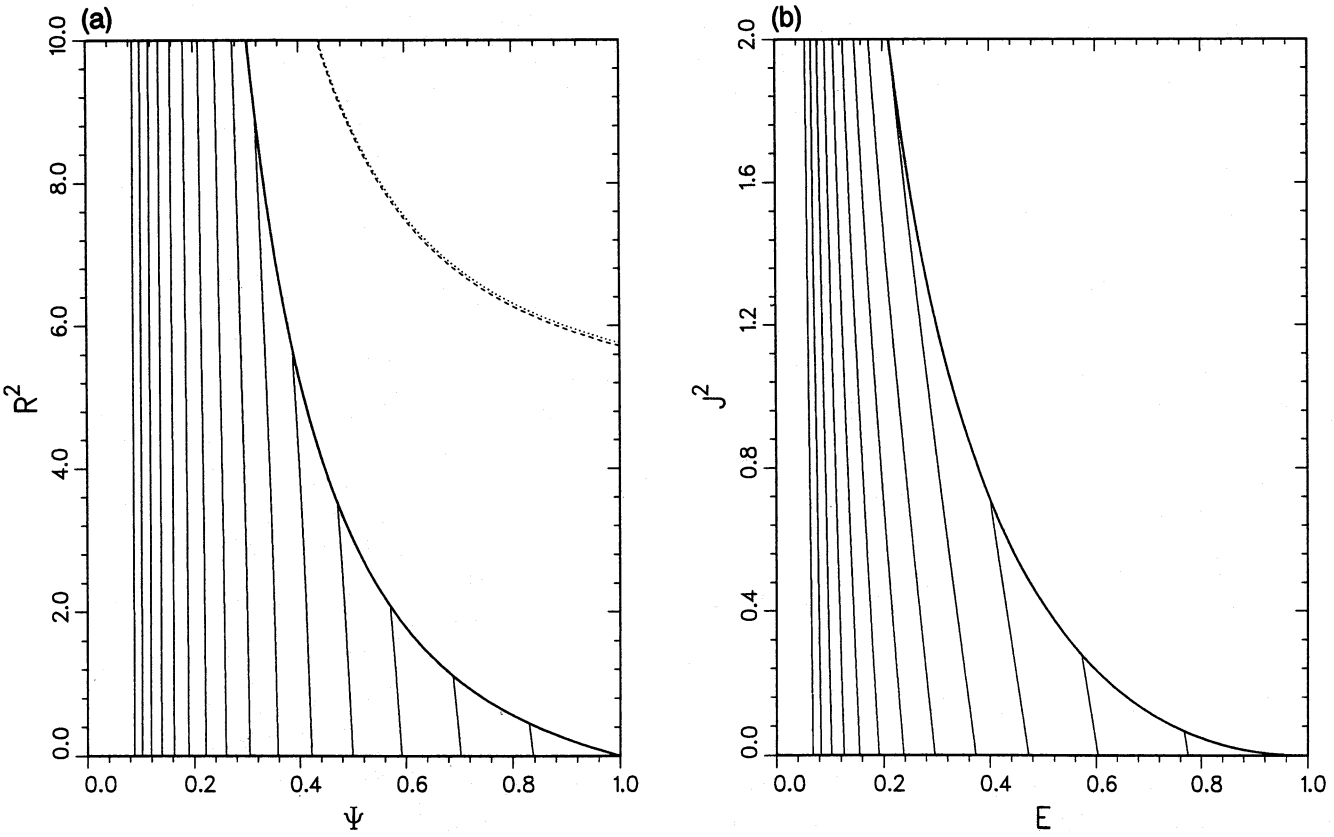


**Figure 11.** Same as Fig. 10 but for a Satoh model with $b/a = 10$, and with successive contour levels differing by factors of 0.4.

The contour needed to obtain the distribution function, as with our other oblate models, encloses two real type I singularities, a branch point $\Psi_1$ and a pole $S_1$, at which the square root and the denominator of the density, respectively, vanish. Both lie between $\Psi = E$ and the window $\mathscr{P}$, and are given by the leftmost positive roots of the two instances of equation (4.16). The window $\mathscr{P}$ lies to the left of any other positive root, should any exist. There may be other real positive zeros of the denominator, even when there are no other real branch points, because the latter are given by an equation (4.16) with a larger and positive $\chi$ (see Fig. 9b). Because $\Psi_1$ and $S_1$ are the only singularities of $\rho$ enclosed by the contour, it must be kept close enough to the real $\Psi$-axis to avoid enclosing any complex conjugate singularities. Wherever the three branch points lie, the square-root term in $\rho$ must be real for real values of $\Psi$ to the immediate right of $\Psi_1$, and vary continuously along the integration contour.

Densities and distribution functions for two of these models, the two extreme cases for which Satoh gives conventional density contours in his Fig. 2, are displayed in Figs 10 and 11. The $b/a = 0.1$ model of Fig. 10 is highly flattened, while the $b/a = 10.0$ model of Fig. 11 is close to spherical. The contours of $f$ again reflect the trends of those of $\rho$ in exaggerated form.

## 5 INFINITE MASS MODELS

The gravitational potential $\Psi$ now has no lower bound and tends to $-\infty$ at large distances. The fundamental integral equation (2.1) is modified to

$$\rho = \frac{2\pi}{R}\int_{-\infty}^{\Psi} \mathrm{d}E \int_0^{2R^2(\Psi - E)} \frac{f(E, J^2)}{\sqrt{J^2}}\,\mathrm{d}J^2 = \frac{2\pi}{R}\int_0^{2R^2\Psi} \frac{\mathrm{d}J^2}{\sqrt{J^2}} \int_{-\infty}^{\Psi - (J^2/2R^2)} f(E, J^2)\,\mathrm{d}E, \tag{5.1}$$

with integration over triangles of infinite extent. The domain $\boldsymbol{F}$ extends infinitely far to the left, but is still bounded above by an envelope $\mathscr{E}$, and the window $\mathscr{P}$ associated with any $(E, J^2)$-point of $\boldsymbol{F}$ is constructed in the same manner. The contour integral solution becomes

$$f(E, J^2) = \frac{1}{4\pi^2 \mathrm{i}\sqrt{2}}\,\frac{\partial}{\partial E}\int_{-\infty}^{[\Psi_{\mathrm{env}}(E)+]} \frac{\mathrm{d}\Psi}{(\Psi - E)^{1/2}}\,\rho_1\left[\Psi, \frac{J^2}{2(\Psi - E)}\right]. \tag{5.2}$$

The contour is again a loop around part of the real axis. It still starts and ends at the value of $\Psi$ corresponding to the potential at large distances, but this is now at $\Psi = -\infty$ rather than at $\Psi = 0$. The alternative formulae (3.3) and (3.4) also apply with the modified path.

In Section 5.1 we apply our contour integral solution to rotating matter with Binney's (1981) logarithmic potential. In Section 5.2 we verify that the contour integral solution (5.2) satisfies the modified integral equation (5.1). There are significant differences between the justification given in this section and that given earlier, for the finite mass case, in Section 3.4.

### 5.1 Application to Binney's logarithmic potential

We write this potential in the form

$$\Psi(R^2, z^2) = -\frac{1}{2} v_0^2 \ln\left(1 + R^2 + \frac{z^2}{q^2}\right), \tag{5.3}$$

where $v_0$ is the constant circular velocity in the equatorial plane at large distances, $q$ is the axial ratio of the spheroidal equipotentials, and units in which the core radius is unity are used. The potential (5.3) is generated by the density

$$\rho(\Psi, R^2) = \frac{v_0^2}{4\pi G q^2}\left\{2[(1-q^2)R^2 + 1]\exp\left(\frac{4\Psi}{v_0^2}\right) + (2q^2 - 1)\exp\left(\frac{2\Psi}{v_0^2}\right)\right\} \tag{5.4}$$

(Evans 1993). Although Evans used Lynden-Bell's (1962) method to find the distribution function, ours can also be used. Both methods are unnecessarily elaborate in this instance because the integral equation (5.1) has elementary solutions

$$f = J^{2k} \mathrm{e}^{aE}, \qquad \rho = \left(\frac{2}{a}\right)^{k+(3/2)} \pi\Gamma\left(k + \frac{1}{2}\right) R^{2k} \mathrm{e}^{a\Psi}, \qquad \text{for } k + \frac{1}{2} > 0, \qquad a > 0, \tag{5.5}$$

for which the dependence of $f$ on $E$ and $J^2$ is identical to that of $\rho$ on $\Psi$ and $R^2$. These solutions were published first in Miller (1982), although they were known earlier to Toomre (1982). They are the analogues for the infinite mass case of Fricke's (1952) elementary solutions (equation A1) for the finite mass case. The density (5.4) and the distribution function of Evans' equation (2.4) are simply sums of three of the elementary solutions (5.5).

The contour integral method is useful for calculating the odd part $f_{\mathrm{odd}}(E, J)$ of the distribution function that corresponds to some assumed rotational velocity $\langle v_\phi \rangle$ field. As Lynden-Bell (1962) noted, equation (2.1) or (5.1) becomes an equation for $Jf_{\mathrm{odd}}(E, J)$, rather than $f(E, J^2)$, if $\rho R\langle v_\phi \rangle$ replaces $\rho$ on the left-hand side. One of the rotation laws considered by Evans (1993) is

$$\langle v_\phi \rangle = \frac{v_* R^2}{R_*^2 + R^2}, \tag{5.6}$$

where $v_*$ and $R_*$ are constant velocity- and length-scales respectively. We shall suppose that this rotation law applies to the whole density (5.4) rather than just to the simpler luminous component considered by Evans. The contour integral formula then gives the expression

$$f_{\mathrm{odd}}(E, J) = \frac{v_* J^2 \,\mathrm{sgn}(J)}{8\pi^2 \mathrm{i}} \int_{-\infty}^{(E+)} \frac{\mathrm{d}\Psi}{(\Psi - E)[J^2 + 2R_*^2(\Psi - E)]} \rho_{11}\left[\Psi, \frac{J^2}{2(\Psi - E)}\right] \tag{5.7}$$

for the odd part of the distribution function. The loop contour encloses a simple pole at $\Psi = E - J^2/2R_*^2$ and a double pole at $\Psi = E$ with the $\rho$ of equation (5.4), and a residue calculation gives

$$f_{\mathrm{odd}}(E, J) = \frac{v_* \,\mathrm{sgn}(J)}{4\pi^2 G q^2 v_0^2}\left\{8[1 - (1-q^2)R_*^2]\left[1 - \exp\left(-\frac{2J^2}{R_*^2 v_0^2}\right)\right]\exp\left(\frac{4E}{v_0^2}\right) + 16(1-q^2)\frac{J^2}{v_0^2}\exp\left(\frac{4E}{v_0^2}\right)\right. \tag{5.8}$$

$$\left. + (2q^2 - 1)\left[1 - \exp\left(\frac{-J^2}{R_*^2 v_0^2}\right)\right]\exp\left(\frac{2E}{v_0^2}\right)\right\}.$$

### 5.2 Justification of the contour integral solution

This justification at first proceeds like that of Section 3.4. We substitute the modified contour integral solution (5.2) into the second form of the integral equation (5.1). We carry out the integration with respect to $E$, and require that the density tends to

zero sufficiently rapidly at large distances that

$$\lim_{E\to-\infty}\int_{-\infty}^{[\Psi_{\rm env}(E)+]}\frac{{\rm d}\Phi}{(\Phi-E)^{1/2}}\rho_1\left[\Phi,\frac{J^2}{2(\Phi-E)}\right]=0. \tag{5.9}$$

The same change of variables and readjustment of the contour as those of Section 3.4 reduce the right-hand side of equation (5.1) to

$$\frac{1}{2\pi{\rm i}}\int_{-\infty}^{\Psi}\frac{{\rm d}B}{(\Psi-B)^{1/2}}\int_{-\infty}^{(\Psi+)}\frac{{\rm d}\Phi}{(\Phi-B)^{1/2}}\rho_1\left[\Phi,R^2\left(\frac{\Psi-B}{\Phi-B}\right)\right]. \tag{5.10}$$

Thereafter the argument is different. We cannot interchange the orders of the integration in the integral (5.10) because that would lead to a divergent inner integral. Instead, we change the inner variable of integration from $\Phi$ to $s$ and the outer from $B$ to $b$, where

$$s=\frac{\Phi-B}{\Psi-B},\qquad b=B-\Psi, \tag{5.11}$$

to obtain

$$\frac{1}{2\pi{\rm i}}\int_{-\infty}^{0}{\rm d}b\int_{-\infty}^{(1+)}\frac{{\rm d}s}{s^{1/2}}\rho_1\left[\Psi+b(1-s),\frac{R^2}{s}\right]. \tag{5.12}$$

The next step is to change the inner path of integration from $\int_{\infty}^{(1+)}$ to $\int_{-\infty}^{(s_0+)}$ for some fixed $s_0$ for which $0<s_0<1$. The validity of this step depends on the analyticity properties of $\rho$. We again assume that $\rho(\Psi, R^2)$ is an analytic function of both of its arguments throughout its physically relevant domain $\boldsymbol{P}$. The main difference in the domain $\boldsymbol{P}$ from that shown in Fig. 3(a) is that it has no finite left boundary but now extends to $-\infty$ in $\Psi$. The rectangle $\boldsymbol{R}$ that we now need to construct, for any interior point $(\Psi, R^2)$ of $\boldsymbol{P}$, is a semi-infinite one which lies entirely in $\boldsymbol{P}$ and has an upper right vertex at $(\Psi, R_0^2)$. Define $s_0=R^2/R_0^2$. The point $[\Psi+b(1-s), R^2/s]$, with arguments as in the integral (5.12), lies within this semi-infinite rectangle for any real $s$ in $s_0\le s\le 1$ and any real $b$ in $-\infty<b\le 0$. By the same argument as in Section 3.4, the integrand of (5.12) is also an analytic function in an open set $\boldsymbol{R}^+$ of $\boldsymbol{C}^2$ containing $\boldsymbol{R}^+$, and hence for values of $s$ in a neighbourhood of the real $s$-axis between $s_0$ and 1. This analyticity allows us to shrink the $z$-path of integration to a loop around $s_0<1$ on which ${\rm Re}(s)<1$ everywhere. The significance of this last step is that it allows us to use the simple $\rho_1$ form of the integrand to perform the outer integration with respect to $b$ explicitly. There is no contribution from the $b=-\infty$ limit provided that $\rho\to 0$ as ${\rm Re}(\Psi)\to-\infty$, as it does for the exponentially decaying densities of Section 5.1, and the result is

$$\frac{1}{2\pi{\rm i}}\int_{-\infty}^{(s_0+)}\frac{{\rm d}s}{s^{1/2}(1-s)}\rho\left(\Psi,\frac{R^2}{s}\right). \tag{5.13}$$

The integrand of (5.13) has a simple pole at $s=1$ which now lies outside the looped path of integration. Provided that $\rho(\Psi, R^2/s)$ has no other singularities as a function of $s$ outside the looped path, as is the case with the densities discussed in Section 5.1, a final change of variables to $t=1/s$ can be made. This transforms the contour integral to

$$\frac{1}{2\pi{\rm i}}\oint\frac{{\rm d}t}{t^{1/2}(t-1)}\rho(\Psi,R^2{\rm t}), \tag{5.14}$$

with a finite closed loop path which starts and ends at $t=0$, the image of $s=\infty$, and which encircles the pole at $t=1$ in the positive sense. Cauchy's Residue Theorem with the residue from this single enclosed pole at $t=1$ evaluates the integral (5.14) as $\rho(\Psi, R^2)$, so that the correct density is again recovered from the right-hand side of equation (5.1).

## 6 CONCLUSION

Our main result is a contour integral formula for the calculation of a classical two-integral distribution function for an axisymmetric system. It is given in equation (3.1) for systems of finite mass, and in equation (5.2) for systems of infinite mass. It is the two-integral analogue of Eddington's (1916) real integral formula for the one-integral distribution function of a spherical system. It is derived directly from the density, and the basic procedure is simple enough to be feasible with complicated densities. Our method will generally require the numerical evaluation of a path integral. This evaluation is much simpler and more

accurate than any direct numerical solution of either of the basic integral equations of the first kind, (2.1) or (5.1), which must be solved to determine the distribution function for a specified density.

The first basic requirement of our method is an analytical axisymmetric potential $\Psi$. This potential defines the structure of the $(\Psi, R^2)$ coordinate system in which the density $\rho$ must be expressed, the forms of the domains $\boldsymbol{P}$ of $\rho$ and $\boldsymbol{F}$ of $f$, and the contour of integration. The second basic requirement is an analytic density $\rho(\Psi, R^2)$. Although this is the self-consistent density in each of our examples, it does not have to be, because no requirement of self-consistency is incorporated into the basic integral equations that we solve.

We have been able to solve explicitly for $z^2$ in terms of $\Psi$ and $R^2$ in the three finite mass models which we analysed in detail in Sections 3.2, 4.1 and 4.2. This simplifies the analysis, but we do not believe it to be essential. All that is necessary is the ability to evaluate the density $\rho$, given $\Psi$ and $R^2$, for real arguments in the domain $\boldsymbol{P}$, and for the analytic continuation into the complex $\Psi$-plane that is necessary for the evaluation of $\rho$ on the contour of integration. Such evaluations will, at least sometimes, be possible when the representation $\rho(\Psi, R^2)$ is known only implicitly.

The perceptive reader may have noted that, although we located all the singularities of the three finite mass models, we ultimately evaluated $f$ numerically, rather than analytically, by integration along a path whose placement is defined in terms of the window $\mathscr{P}$, and not in terms of where the singularities are. For the practical consideration of achieving good numerical accuracy, the contour should avoid coming close to enclosed pole singularities at which the integrand becomes infinite, but the detours must not be so large as to enclose singularities, such as the complex poles or branch points of Satoh's model, which must lie outside the contour. The accuracy and validity of a numerical routine for the calculation of $f$ can be checked numerically, by testing whether it reproduces the correct density when substituted back into the real line integral (2.6) or its infinite mass equivalent.

We have shown directly that our solutions satisfy the basic integral equations. Our justifications do rely on certain assumptions concerning the nature of the singularities of the density $\rho$, such as those described in Section 3.3. These assumptions are valid for our examples, which is another reason for our detailed discussion of their singularities, but we have given no explanation as to why this should always be so. It is conceivable that subsequent work will show that we have not been sufficiently imaginative as to the variety of singularity behaviour that can arise in physical applications, in which case our justification analyses will need to be re-examined.

The most noteworthy feature of our computed distribution functions is the resemblance between the dependence of $f$ on $E$ and $J^2$ and that of $\rho$ on $\Psi$ and $R^2$. This resemblance is not surprising in view of its occurrence in the elementary solution (5.5), and to a reduced extent in Fricke's elementary solution (A1). The fact that this resemblance has not been noticed before is presumably due to the fact that previous workers have omitted to plot $\rho$ as a function of $\Psi$ and $R^2$, despite the fact that such plots are simple to generate.

Most of the currently known two-integral axisymmetric distribution functions, as listed in Section 1, can be found by Fricke's method. Fricke's method requires that $\rho(\Psi, R^2)$ be expanded as a doubly infinite series in $\Psi$ and $R^2$, and therefore implicitly requires that $\rho$ be analytic. Our contour integral formula is always available as an alternative in cases for which Fricke's method can be used; the interrelationship of the two methods is discussed in Appendix A. Because circles of convergence of power series may impose restrictions on Fricke's method which the contour integral method can circumvent, Fricke's method is not always available as an alternative to our contour integral method. When both methods can be used, the contour integral is likely to be preferable for both computational and analytical purposes unless the density $\rho(\Psi, R^2)$ is a finite polynomial. When the density is as complicated as in the general case of the flattened isochrone density (4.7), Fricke's method is probably infeasible, even if theoretically possible. Dejonghe & de Zeeuw (1988) did find a finite integral representation for the distribution function of the Kuzmin–Kutuzov model, which they had initially found by Fricke's method in series form. This success depended upon the fortuitous availability, in Gradshteyn & Ryzhik (1980), of an integral representation of a generalized hypergeometric function and is special to that model. Our integral representations arise automatically, and require neither skills with special functions and integral tables, nor densities of any specially simple form.

The examples presented here for both finite and infinite mass systems show that the new contour integral method is both powerful and adaptable. We are actively pursuing further applications of it, some in conjunction with Wyn Evans and Tim de Zeeuw. We have found that our method is fully capable of handling cusped density distributions with infinities at their centres. Such infinities lie outside the contour of integration at the maximum central value of the potential, but the contour is squeezed towards the central infinity as $E$ tends towards this maximum.

Like other contour integral formulae, ours may prove to be useful for obtaining asymptotic approximations for $f$. We have not yet explored this possibility.

## ACKNOWLEDGMENTS

This research was supported in part by the National Science Foundation through Grant DMS 9001404 and by NASA through the Florida Space Grant Consortium Interinstitutional Space Research Program Grant NGT-40015. CH wishes to thank Sterrewacht Leiden for their hospitality during a sabbatical year's visit, and NWO, the Netherlands Organization for Scientific

Research, for a Bezoekersbeurs which supported this visit. It is also a pleasure to thank Tim de Zeeuw and Wyn Evans for stimulating discussions. Some of the computations reported here were supported by Florida State University through the SUN system of the Mathematics Department and the allocation of supercomputer resources. Others were performed on the STRWCHEM system at Leiden University.

## REFERENCES

Binney J. J., 1981, MNRAS, 196, 455
Binney J., Tremaine S., 1987, Galactic Dynamics. Princeton Univ. Press, Princeton
Courant R., Hilbert D., 1953, Methods of Mathematical Physics, Vol. 1. Interscience Publishers, New York, Ch. 3
Davies B., 1978, Integral Transforms and Their Applications. Springer-Verlag, Berlin
Dejonghe H., 1986, Phys. Rep., 133, 218
Dejonghe H., 1987, MNRAS, 224, 13
Dejonghe H., de Zeeuw P. T., 1988, ApJ, 333, 90
de Zeeuw P. T., 1987, in de Zeeuw P. T., ed., Proc. IAU Symp. 127, Structure and Dynamics of Elliptical Galaxies. Reidel, Dordrecht, p. 271
Eddington A. S., 1916, MNRAS, 76, 572
Erdelyi A., Magnus W., Oberhettinger F., Tricomi F. G., 1953, Higher Transcendental Functions, Vol. 1. McGraw-Hill, New York
Evans N. W., 1993, MNRAS, 260, 191
Evans N. W., de Zeeuw P. T., Lynden-Bell D., 1990, MNRAS, 244, 111
Fricke W., 1952, Astron. Nachr., 280, 193
Geigant E., 1991, Diplomarbeit, Ludwig-Maximilians-Universität, München
Gradshteyn I. S., Ryzhik I. M., 1980, Table of Integrals, Series, and Products, 2nd edn. Academic Press, New York
Hunter C., 1975, AJ, 80, 783
Kalnajs A. J., 1976, ApJ, 205, 751
Kuzmin G. G., 1956, AZh, 33, 27
Kuzmin G. G., Kutuzov S. A., 1962, Bull. Abastumani Astrophys. Obs., 27, 82
Lake G., 1981, ApJ, 243, 111
Lindblad B., 1934, MNRAS, 94, 231
Lynden-Bell D., 1962, MNRAS, 123, 447
Miller R. H., 1982, ApJ, 254, 75
Miyamoto M., 1971, PASJ, 23, 21
Nagai R., Miyamoto M., 1976, PASJ, 28, 1
Satoh C., 1980, PASJ, 32, 41
Stieltjes T. J., 1894, Ann. Fac. Sci. Toulouse, 8, 1
Titchmarsh E. C., 1937, An Introduction to the Theory of Fourier Integrals. Oxford Univ. Press, Oxford, Ch. 11
Toomre A., 1963, ApJ, 138, 385
Toomre A., 1982, ApJ, 259, 535
Whittaker E. T., Watson G. N., 1927, A Course of Modern Analysis, 4th edn. Cambridge Univ. Press, Cambridge
Widder D. V., 1941, The Laplace Transform. Princeton Univ. Press, Princeton, Ch. 8

## APPENDIX A: FRICKE'S SOLUTIONS AND METHOD

Fricke's (1952) elementary solutions of the integral equation (2.1) are

$$f=E^jJ^{2k}, \qquad \rho=\frac{2^{k+(3/2)}\pi\Gamma(j+1)\Gamma[k+(1/2)]\Psi^{j+k+(3/2)}R^{2k}}{\Gamma[j+k+(5/2)]}, \qquad \text{for } k+\tfrac{1}{2}>0, \qquad j>-1. \tag{A1}$$

His method for finding two-integral distribution functions is to expand $\rho(\Psi, R^2)$ as a double-power series in $\Psi$ and $R^2$, and then apply the solutions (A1). The circles of convergence of such expansions correspond to regions of the complex $\Psi$-plane in which the density $\rho[\Psi, J^2/2(\Psi-E)]$ of our contour integral is analytic, and hence in which its path may be placed. Consequently, densities for which Fricke's method is successful are densities for which our contour integral can also be used. On the other hand, the contour integral method can work in cases in which Fricke's power series diverge in part of the physical domain ***P***, as the following example illustrates.

Dejonghe & de Zeeuw (1988) applied Fricke's method to the Kuzmin–Kutuzov model. They first expanded the density (3.10) in powers of $a\Psi/\sqrt{1-AR^2\Psi^2}$ and then expanded inverse powers of $\sqrt{1-AR^2\Psi^2}$ in powers of $AR^2\Psi^2$. The double expansion is valid provided that the density $\rho(\Psi, R^2)$ is analytic in the intersection of the two circles of convergence

$$a^2|\Psi^2|<|1-AR^2\Psi^2|, \qquad |AR^2\Psi^2|<1. \tag{A2}$$

The density $\rho[\Psi, J^2/2(\Psi-E)]$ is then analytic in the intersection of the regions of the complex $\Psi$-plane that are defined by the inequalities

$$a^2|\Psi^2|<\left|1-\frac{AJ^2\Psi^2}{2(\Psi-E)}\right|, \qquad \left|\frac{AJ^2\Psi^2}{2(\Psi-E)}\right|<1. \tag{A3}$$

These regions are annular when the parameter $A$ lies in the range $-1<A<1$. The first annulus contains both $O$ and $E$, but excludes an inner core which cuts out the segment of the real axis between $S_1$ and $S_1^+$, the root of the equation $AJ^2\Psi^2/2(\Psi-E)=1+a^2\Psi^2$ that lies between $E$ and $S_1$. (The interested reader should add to Figs 4a and 5a.) The second annulus contains $O$, but $E$ lies within its excluded inner core. This excluded core cuts out the segment of the real axis from $\Psi_1$ to $\Psi_3$, where $\Psi_3$ is a positive root of $AJ^2\Psi^2/2(\Psi-E)=-1$. The two annuli always have a common annular intersection for the parameter range $-1<A<1$, and the path of our contour integral could be taken to lie in this common annulus.

For $A<-1$, Fricke's method fails for values of $E$ and $J^2$ for which $2AEJ^2<-1$ (Dejonghe & de Zeeuw, section IVc), when the expansion of $\rho$ is needed for arguments for which $|AR^2\Psi^2|>1$ and it diverges. The geometric picture in the complex $\Psi$-plane is that the region defined by the second of the inequalities (A3) then ceases to be an annulus. The root $\Psi_3$ has disappeared, the excluded inner core has linked up with the excluded outer region, and the second of the inequalities (A3) is not satisfied anywhere on the real $\Psi$-axis to the right of $E$. The contour of our integral must now pass outside the intersection, but the contour integral method still works because its path is not restricted by the inequalities (A3).

## APPENDIX B: INTEGRAL TRANSFORM METHODS

Ever since Lynden-Bell's (1962) use of Laplace transforms, integral transform methods have held the promise of being an effective method of solving the fundamental integral equation (2.1). They have had some subsequent successes (Dejonghe 1986; Hunter 1975; Kalnajs 1976; Evans 1993), and we began this work using them. We derived our contour integral solution with the simplified form $\int_0^{(E+)}$ of its contour using a single Mellin transform. This derivation, which we give in Section B.1, is heuristic. We see no way of making it otherwise, and of thereby deriving a full specification of the integration contour.

We have now become convinced that integral transform methods generally are not the ones to use, which is why we have banished discussion of them to this appendix. We have already shown that one major difficulty for integral transforms is that non-physical singularities of $\rho$ in $(\Psi, R^2)$-space can prevent transforms existing. A way to avoid this difficulty is to set the density to zero outside its physically relevant domain $\boldsymbol{P}$, which will not affect the values of the distribution function in its physically relevant domain $\boldsymbol{F}$. Though simple in principle, this idea may not be so in practice. It is important to realize that we cannot simultaneously set both $f$ and $\rho$ to zero outside their physically relevant domains. Although we could just as well do this to $f$ as to $\rho$, we cannot simultaneously do it to both *and* also require that the integral equation (2.1) be valid for the infinite ranges of arguments that the taking of integral transforms implicitly requires. To set $\rho=0$ outside the physically relevant region and to take the transform imply that $f$ is generally non-zero (and indeed often negative) for non-physical ranges of its arguments.

Because of the usefulness of Fricke's (1952) expansion method, it is natural to expect that an effective way of obtaining further and more general solutions would be to use continuous combinations of his elementary solutions (A1) via a double Mellin transform. Previous successful uses of Mellin transforms for finding distribution functions (Kalnajs 1976; Dejonghe 1986) have all been applications of single, rather than double, Mellin transforms. We shall discuss the use of a double Mellin transform in Section B.2, where we find the distribution function for a simple density component proposed by Dejonghe (1986). Dejonghe found this distribution function by Fricke's expansion method, although its expansion does not converge in all the cases for which it is needed (cf. Appendix A). The double Mellin transform approach sets $\rho$ to zero for non-physical values of $\Psi>1$, and is effective in cases for which the series expansion does not converge. The contrast between the work required in this analysis of a simple density, and that of Section B.2.2 where we apply our contour integral method to the same density, suggests that it will be hard to find problems for which Mellin transform methods are easier than ours. Lastly, in Section B.3, we relate the Stieltjes transform method of Hunter (1975) to our contour integral solution.

### B.1 Heuristic derivation of the contour integral solution via a single Mellin transform

We take a single Mellin transform with respect to $R^2$ of the alternative equation (2.6). We denote Mellin transforms, with transform variable $s$, by capital letters, so that of $\rho$ is

$$P(\Psi, s)=\int_0^\infty (R^2)^{s-1}\rho(\Psi, R^2)\,\mathrm{d}R^2. \tag{B1}$$

The transform of equation (2.6) is

$$\frac{\partial P(\Psi, s)}{\partial \Psi}=\frac{\pi}{2^{s-(3/2)}}\int_0^\Psi \frac{F(E, s)\,\mathrm{d}E}{(\Psi-E)^{s+(1/2)}}, \tag{B2}$$

where

$$F(E, s)=\int_0^\infty (J^2)^{s-1}f(E, J^2)\,\mathrm{d}J^2 \tag{B3}$$

is the Mellin transform of $f(E, J^2)$ with respect to $J^2$. The transform $P(\Psi, s)$ exists for $\mathrm{Re}(s)>0$ for a density which is finite at $R^2=0$ and which vanishes when $R^2$ exceeds some $\Psi$-dependent maximum value. Equation (B2) can be solved, provided also that $\mathrm{Re}(s)<1/2$, to give

$$F(E, s)=\frac{\cos \pi s}{2\pi^2}\frac{\partial}{\partial E}\int_0^E [2(E-\Psi)]^{s-(1/2)}\frac{\partial P(\Psi, s)}{\partial \Psi}\,\mathrm{d}\Psi. \tag{B4}$$

The cos $\pi s$ term that occurs here and in earlier work is a sign that the inversion calculation needs to make use of values of the density for complex arguments. Dejonghe (1986) handles this inversion using a theorem from Davies (1978). Davies's theorem applies here to functions of $R^2$ that are holomorphic throughout the complex $R^2$-plane, except for the negative real $R^2$-axis. This restrictive requirement is similar to one encountered in the Stieltjes transform approach (see Section B.3). Our new way of treating this awkward cos $\pi s$ term is to absorb it into the conversion of the real integral of equation (B4) into the contour integral

$$F(E,s)=\frac{1}{4\pi^2 i\sqrt{2}}\frac{\partial}{\partial E}\int_0^{(E+)}\frac{d\Psi}{(\Psi-E)^{1/2}}[2(\Psi-E)]^s\frac{\partial P(\Psi,s)}{\partial\Psi}. \tag{B5}$$

The formal Mellin inversion of this equation is simple, because the variable $s$ now appears explicitly only as a power, and gives the contour integral solution

$$f(E,J^2)=\frac{1}{4\pi^2 i\sqrt{2}}\frac{\partial}{\partial E}\int_0^{(E+)}\frac{d\Psi}{(\Psi-E)^{1/2}}\rho_1\left[\Psi,\frac{J^2}{2(\Psi-E)}\right], \tag{B6}$$

although with the simplified version of the contour of integration, which is not always valid. The inversion is only formal because we have performed it for arguments that lie on a complex contour, and cannot be justified directly without also imposing analyticity requirements on the density that are unnecessarily restrictive.

### B.2 Double Mellin transforms

Following Kalnajs's (1976) work for the disc case, we define the double Mellin transform of $\rho$ as

$$P(s,t)=\int_0^\infty (R^2)^{s-1}\,dR^2\int_0^\infty \Psi^{t-1}\rho(\Psi,R^2)\,d\Psi, \tag{B7}$$

and assume that these infinite integrals converge. The inverse of the transform (B7) is then

$$\rho(\Psi,R^2)=\frac{1}{(2\pi i)^2}\int_{C_1-i\infty}^{C_1+i\infty}\frac{ds}{R^{2s}}\int_{C_2-i\infty}^{C_2+i\infty}\frac{dt}{\Psi^t}P(s,t), \tag{B8}$$

where the real constants $C_1$ and $C_2$ are chosen in such a way that the contours of integration lie in regions for which the double integral of equation (B7) converges. The inversion (B8) is the required representation of $\rho$ in terms of a continuous set of Fricke's elementary solutions (A1). By setting $k=-s$ and $j=s-t-(3/2)$ in these solutions, we obtain the distribution function as

$$f(E,J^2)=\frac{1}{\pi(2\pi i)^2(2E)^{3/2}}\int_{C_1-i\infty}^{C_1+i\infty}\left(\frac{2E}{J^2}\right)^s ds\int_{C_2-i\infty}^{C_2+i\infty}\frac{dt}{E^t}\frac{\Gamma(1-t)P(s,t)}{\Gamma[s-t-(1/2)]\Gamma[(1/2)-s]}, \tag{B9}$$

i.e. as a double inverse Mellin transform of some multiple of the double Mellin transform of the density. It may be necessary to modify the definition of $\rho$ to meet the convergence requirements of the Mellin transforms.

#### *B.2.1 Dejonghe's building-block density by a double Mellin transform*

Dejonghe (1986) introduced the density

$$\rho(\Psi,R^2)=\Psi^\alpha(1-AR^2\Psi^2)^\beta, \tag{B10}$$

where $\alpha$, $\beta$ and $A$ are constants. He, and then Dejonghe & de Zeeuw (1988), used it as a building block for the determination of other distribution functions. Certain restrictions need to be placed on its constants. The fact that the density falls to zero sufficiently rapidly at large distances to give a finite total mass requires that $\alpha>3$. To avoid the occurrence of negative values of the second factor of $\rho$ in the physically significant range $0\le R\Psi\le 1$, it is necessary to require that either $0<A\le 1$ or $A<0$. The two possibilities are the same as the oblate and prolate cases of the Kuzmin–Kutuzov model of Section 3.2. They again require somewhat different treatment, and we shall discuss only the $A<0$ prolate case in detail.

The density (B10) does not itself define a physical domain $P$. However, the definition

$$\rho(\Psi,R^2)=\begin{cases}\Psi^\alpha(1-AR^2\Psi^2)^\beta, & \text{for } 0\le\Psi\le 1;\\ 0, & \text{otherwise,}\end{cases} \tag{B11}$$

which modifies $\rho$ outside the region $0 \le \Psi \le 1$ only, and hence outside $\boldsymbol{P}$, is more convenient. It allows us to evaluate the Mellin transform of $\rho$ explicitly, provided that $-\beta > \mathrm{Re}(s) > 0$ and $\alpha + \mathrm{Re}(t-2s) < 0$, as

$$P(s,t) = \frac{\Gamma(s)\Gamma(-\beta-s)}{(\alpha+t-2s)\Gamma(-\beta)(-A)^s}. \tag{B12}$$

This is analytic in the right half-space region $\mathrm{Re}(t) > 2\mathrm{Re}(s) - \alpha$ for which the integrals converge. However, the Mellin transform of $f$, contained in the right-hand side of equation (B9), is *not* analytic in any right half-space in the complex $t$-plane, contrary to a statement by Kalnajs (1976). This is because the simple poles given by the $\Gamma(1-t)$ term at $t = N$, for all positive integers $N$, stretch arbitrarily far to the right in the complex $t$-plane due to the fact (discussed earlier) that, unlike $\rho$, $f$ does not generally vanish outside its physically relevant domain. Its Mellin transform is valid in a strip in the complex $t$-plane only (Davies 1978), and it is necessary that $C_2 < 1$ in order for the poles of $\Gamma(1-t)$ all to lie to the right of the $t$-path of integration in equation (B9). These poles contribute to the value of $f$ in the non-physical range $E > 1$, as is seen by evaluating the inner $t$-integration of equation (B9) by closing the contour with a large right semi-circle. (If any of the poles lay to the left, they would give unacceptably singular behaviour at low energies.) For the physical range $E < 1$, the inner $t$-integration of equation (B9) is evaluated by closing the contour with a large left semi-circle. This encloses only the simple pole at $t = 2s - \alpha$, and gives the evaluation

$$f(E,J^2) = \frac{(2E)^{\alpha-(3/2)}}{\pi^{3/2}(2\pi\mathrm{i})} \int_{C_1-\mathrm{i}\infty}^{C_1+\mathrm{i}\infty} \frac{\mathrm{d}s}{(-2AEJ^2)^s} \frac{\Gamma(-\beta-s)\Gamma(s)\Gamma\{[(1+\alpha)/2]-s\}\Gamma\{[(2+\alpha)/2]-s\}}{\Gamma(-\beta)\Gamma[(1/2)-s]\Gamma[\alpha-(1/2)-s]}. \tag{B13}$$

The new integrand also has poles that stretch to infinity both left and right. Those that extend to the right come from the $\Gamma(1-t)$ term, which we have expanded using the duplication formula. They cause generally non-zero values of $f$ for all $EJ^2$. The path of integration must pass to the right of the simple poles of $\Gamma(s)$ and to the left of those of $\Gamma(-\beta-s)$ because of the earlier condition $-\beta > \mathrm{Re}(s) > 0$. It must pass to the left of the other simple poles at $s = (N+\alpha)/2$ to avoid unacceptably singular terms.

Integral (B13) matches the definition of a generalized hypergeometric function as a Mellin–Barnes integral. Using formulae (5.3.1), (5.3.2) and (5.6.1) of Erdelyi et al. (1953, Vol. 1), we obtain the formula

$$f(E,J^2) = \frac{E^{\alpha-(3/2)}\Gamma(\alpha+1)}{(2\pi)^{3/2}\Gamma[\alpha-(1/2)]} {}_3F_2\left(\frac{1+\alpha}{2}, \frac{2+\alpha}{2}, -\beta; \frac{1}{2}, \alpha-\frac{1}{2}; 2AEJ^2\right), \tag{B14}$$

which is the same generalized hypergeometric function that Dejonghe (1986) obtained by Fricke's method following a binomial expansion of equation (B10). The range $2AEJ^2 < -1$ for which Dejonghe's infinite series does not converge can be physically significant in this case, and a more general formula, such as that of equation (B13) or the real integral (B18) below, is then needed.

A similar, though not identical, treatment of the oblate case can be based on the redefinition

$$\rho(\Psi, R^2) = \begin{cases} \Psi^\alpha(1-AR^2\Psi^2)^\beta, & \text{if } 0 \le (R\Psi)^2 \le A^{-1}, \quad 0 \le \Psi \le 1; \\ 0, & \text{otherwise.} \end{cases} \tag{B15}$$

### *B.2.2 Dejonghe's building-block density by the contour integral method*

Equation (3.3) applied to the density (B10) gives the contour integral

$$f(E,J^2) = \frac{1}{4\pi^2\mathrm{i}\sqrt{2}} \frac{\partial^2}{\partial E^2} \int_0^{[\Psi_{\mathrm{env}}(E)+]} \frac{\Psi^\alpha}{(\Psi-E)^{1/2}} \left[1 - \frac{AJ^2\Psi^2}{2(\Psi-E)}\right]^\beta \mathrm{d}\Psi \tag{B16}$$

for both the prolate and oblate cases. It has the same two additional branch points $\Psi_1$ and $\Psi_2$ as the Kuzmin–Kutuzov model of Section 3.2, and cuts are chosen in the same way as there. Because there are no other complicating singularities, we can choose the contour to be the circle centre $\Psi = E$ and radius $E$, using the representation

$$\Psi = E + E\,\mathrm{e}^{\mathrm{i}\theta}, \qquad -\pi \le \theta \le \pi, \tag{B17}$$

with angular parameter $\theta$. This gives

$$f(E,J^2) = \frac{1}{4\pi^2} \frac{\partial^2}{\partial E^2} \left\{(2E)^{\alpha+(1/2)} \int_{-\pi}^{\pi} \left(\cos\frac{\theta}{2}\right)^\alpha \cos\left[\frac{(\alpha+1)\theta}{2}\right] \left(1 - 2AEJ^2\cos^2\frac{\theta}{2}\right)^\beta \mathrm{d}\theta\right\}. \tag{B18}$$

This integral representation of $f$ differs significantly from the one that Dejonghe & de Zeeuw (1988) used in deriving their closed form for the distribution function of the Kuzmin–Kutuzov (1962) model. The $2AEJ^2$ term occurs in the $\alpha$th power in their form,

rather than in a $\beta$th power as in equation (B18). Hence it seems unlikely that the equivalence of the two representations can be demonstrated merely by a change of variable of integration.

### B.3 The Stieltjes transform

Hunter (1975) showed that Lynden-Bell's (1962) double Laplace transform method can be cast in the form of an inversion of a Stieltjes transform. A simple and direct statement of this result is that, if the density can be represented in the form

$$\rho(\Psi, R^2)=\frac{1}{R}\int_0^\infty \frac{K(\Psi, p)}{p+R^{-2}}\,\mathrm{d}p, \tag{B19}$$

for some function $K(\Psi, p)$, differentiable with respect to $\Psi$ and which tends to zero as $\Psi\to 0$, then the distribution function is given by

$$f(E, J^2)=\frac{1}{2\pi\sqrt{J^2}}\,\frac{\partial}{\partial E}\left\{\int_0^E K_1\left[\Phi, \frac{2(E-\Phi)}{J^2}\right]\mathrm{d}\Phi\right\}. \tag{B20}$$

This real integral solution can be verified by direct substitution into the second form of the right-hand side of equation (2.1). The verification involves only simple manipulations with real integrals, and so is much more straightforward than that of Section 3.4. However, the representation (B19) requires that $R\rho$ be an analytic function $R^{-2}$ in the whole of the complex $R^2$-plane except for its negative real axis. This requirement is overly restrictive, as the examples discussed in this paper clearly show. When it and the conditions for obtaining the function $K$ by Stieltjes's (1894) inversion formula in terms of the discontinuity of $\rho$ across the negative real $R^2$-axis (Titchmarsh 1937; Widder 1941) are fulfilled, we have

$$K(\Psi, p)=\frac{1}{2\pi\mathrm{i}}\left[\frac{1}{(p\mathrm{e}^{-\pi\mathrm{i}})^{1/2}}\,\rho\left(\Psi, \frac{1}{p\mathrm{e}^{-\pi\mathrm{i}}}\right)-\frac{1}{(p\mathrm{e}^{\pi\mathrm{i}})^{1/2}}\,\rho\left(\Psi, \frac{1}{p\mathrm{e}^{\pi\mathrm{i}}}\right)\right]. \tag{B21}$$

The simple form (B6) of our contour integral solution is obtained when this relation is substituted into equation (B20). The Stieltjes transform solution can therefore be regarded as a precursor of the contour integral solution. It indicated that a solution could be found fairly directly from the prescribed density and without the use of tomes of integral transforms. The restrictions that have so far hampered its usefulness have now been removed by the contour integral method.

## APPENDIX C: ANISOTROPIC DISTRIBUTION FUNCTIONS FOR DISCS AND SPHERES

We now adapt our contour integral method to the related problems of finding two-integral distribution functions for discs and spheres with specified potentials and densities. The second integral in the spherical case is the square of the total angular momentum, rather than that of one of its components. In both cases, integration of $f$ over velocity space gives an expression for the density in terms of the potential and the square of a radial coordinate. However, that potential is now a unique function of the radial coordinate, so the physical problem specifies the density only on a curve in the $(\Psi, R^2)$-plane. Some representation of the density in the rest of a domain $\boldsymbol{P}$ then has to be selected to obtain a problem analogous to the axisymmetric one. The many ways of doing this generate many possible distribution functions. The resulting integral equations for both cases have elementary solutions of Fricke's (1952) type, and these have been used by several workers to construct distribution functions (Miyamoto 1971; Kalnajs 1976; Dejonghe 1986). We shall show that there are elementary transformations which reduce both integral equations to the integral equation (2.1) of the axisymmetric case, and hence allow our techniques to be used. We discuss the disc case, with an example, in Section C.1, and the spherical case in Section C.2.

### C.1 Disc-like systems

The basic integral equation of this case is different because of the lower dimensionality of its velocity space. Integration over this two-dimensional space gives the representation

$$\sigma=2\int_0^\Psi \mathrm{d}E\int_0^{2R^2(\Psi-E)}\frac{\mathrm{d}J^2}{\sqrt{J^2}}\,\frac{f(E, J^2)}{\sqrt{2R^2(\Psi-E)-J^2}}=2\int_0^{2R^2\Psi}\frac{\mathrm{d}J^2}{\sqrt{J^2}}\int_0^{\Psi-(J^2/2R^2)}\frac{f(E, J^2)\,\mathrm{d}E}{\sqrt{2R^2(\Psi-E)-J^2}} \tag{C1}$$

for the surface density. To obtain a related axisymmetric problem, we must use the potential to compensate for the different dimensionality of velocity space, and generate a pseudo-volume density $\hat{\rho}$ from the surface density $\sigma(\Psi, R^2)$ according to the definition

$$\hat{\rho}(\Psi, R^2)=\sqrt{2}\int_0^\Psi \frac{\sigma(\Phi, R^2)\,\mathrm{d}\Phi}{\sqrt{\Psi-\Phi}}. \tag{C2}$$

The same right-hand side as that of equation (2.1) is obtained when the $\sigma$ of equation (C1) is substituted into this definition, orders of integrations are changed, and an elementary integration performed. Hence our contour integral solution applies if the pseudo-density $\hat{\rho}(\Psi, R^2)$ is used.

### *C.1.1 Generalized Miyamoto discs*

We shall now generalize a set of models constructed by Miyamoto (1971) for the Kuzmin–Toomre disc (Kuzmin 1956; Toomre 1963). Its potential is the same $\Psi = GM/\sqrt{1+R^2}$ as that of the Satoh model in its equatorial plane. Miyamoto generated a discrete family of distribution functions by setting

$$\sigma(\Psi, R^2) = \frac{M}{2\pi(1+R^2)^{3/2}} = \frac{M}{2\pi}\Psi^{2m+3}(1+R^2)^m, \tag{C3}$$

where $m$ is an integer, expanding the polynomial in $R^2$, and using Fricke's method. His approach fails for non-integer $m$ when validity of the series expansion in $R^2$ is limited to $|R^2| \le 1$.

Our contour integral method works for non-integer values of $m$. It needs the pseudo-density

$$\hat{\rho}(\Psi, R^2) = \frac{M}{\pi\sqrt{2}} B[2m+4, (1/2)]\Psi^{2m+(7/2)}(1+R^2)^m, \tag{C4}$$

which gives the distribution function as

$$f(E, J^2) = \frac{\Gamma(2m+4)\Gamma(1/2)M}{8\pi^3 \mathrm{i}\Gamma[2m+(5/2)]} \int_0^{(E+)} \frac{\Psi^{2m+(3/2)}[\Psi - E + (1/2)J^2]^m}{(\Psi - E)^{m+(1/2)}} \mathrm{d}\Psi, \tag{C5}$$

with an extra branch point at $\Psi = E - (1/2)J^2$ on the real $\Psi$-axis to the left of $E$. The passage of this extra branch point through $O$ results in some non-smoothness of $f$ across the radial line $E = (1/2)J^2$ in the domain $\boldsymbol{F}$. The magnitude of the discontinuity which occurs when $m$ is not an integer is $O\{[E - (1/2)J^2]^{3m+(5/2)}\}$. The circular contour (B17) with angular variable $\phi = -\theta/2$ can be used to reduce equation (C5) to

$$f(E, J^2) = \frac{\Gamma(2m+4)\Gamma(1/2)ME^{2m+2}}{4\pi^3\Gamma[2m+(5/2)]} \int_{-\pi/2}^{\pi/2} \mathrm{e}^{-\mathrm{i}[m+(5/2)]\phi}[2\cos\phi]^{2m+(3/2)} \left\{\mathrm{e}^{-\mathrm{i}\phi} + \frac{J^2}{2E}\mathrm{e}^{\mathrm{i}\phi}\right\}^m \mathrm{d}\phi. \tag{C6}$$

This integral, which is real because the imaginary part of the integrand is odd in $\phi$, can be used for all values of $J^2/2E$. It can be evaluated in terms of hypergeometric functions using equation (2.4.11) of Erdelyi et al. (1953), from which a required $b^{2\nu}$ factor is missing. The evaluation requires two different cases, and gives

$$f(E, J^2) = \begin{cases} \dfrac{(2m+3)ME^{2m+2}}{4\pi^2} {}_2F_1\left(-m, -2m-2; \dfrac{1}{2}; \dfrac{J^2}{2E}\right), & \text{if } J^2 < 2E; \\ \dfrac{\Gamma(2m+4)ME^{2m+2}}{4\pi^{3/2}\Gamma[m+(1/2)]\Gamma(m+3)} \left(\dfrac{J^2}{2E}\right)^m {}_2F_1\left(-m, \dfrac{1}{2}-m; m+3; \dfrac{2E}{J^2}\right), & \text{if } J^2 > 2E. \end{cases} \tag{C7}$$

Erdelyi et al.'s warning that the second form of equation (C7) is not the analytic continuation of the first should be heeded, and gives a good reason for using the earlier equation (C6) to evaluate $f$. We quote the form (C7) of the distribution function to show its similarity to the ones derived by Dejonghe (1986, 1987) by Mellin transforms for some anisotropic spherical Plummer models.

## C.2 Spherical systems

The problem here is that of determining an isotropic distribution function $f(E, L^2)$, where $L^2$ is now the square of the magnitude of the total angular momentum. Integration over velocity space gives a density

$$\rho = \frac{2\pi}{r}\int_0^{\Psi} \mathrm{dE} \int_0^{2r^2(\Psi - E)} \frac{f(E, L^2)\,\mathrm{d}L^2}{\sqrt{2r^2(\Psi - E) - L^2}} = \frac{2\pi}{r}\int_0^{2r^2\Psi} \mathrm{d}L^2 \int_0^{\Psi - (L^2/2r^2)} \frac{f(E, L^2)\,\mathrm{d}E}{\sqrt{2r^2(\Psi - E) - L^2}} \tag{C8}$$

as a function of $r^2$ and $\Psi$, where $r$ is now a spherical polar coordinate. A modification of the density is needed to convert this problem to an equivalent axisymmetric problem. We define the modified density to be

$$\tilde{\rho}(\Psi, R^2)=\frac{1}{\pi}\int_0^{R^2}\frac{\rho(\Psi, r^2)\,\mathrm{d}r^2}{\sqrt{r^2(R^2-r^2)}}, \tag{C9}$$

the modification now compensating for the difference between the two radial coordinates. Applying the modifying operator of equation (C9) to equation (C8), interchanging orders of integrations, and carrying out the $r^2$-integration, one obtains the integral equation

$$\tilde{\rho}(\Psi, R^2)=\frac{2\pi}{R}\int_0^{\Psi}\mathrm{d}E\int_0^{2R^2(\Psi-E)}\frac{f(E, L^2)\,\mathrm{d}L^2}{\sqrt{L^2}}, \tag{C10}$$

which is formally equivalent to equation (2.1).

## APPENDIX D: SOME SINGULAR DISTRIBUTION FUNCTIONS

Consider distribution functions of the form

$$f(E, J^2)=E^{1/2}g(E)\,\delta(J^2-2\lambda E), \tag{D1}$$

where $\lambda$ is a positive constant and $g$ is some function. Although this $f$ is zero throughout the domain $\boldsymbol{F}$ except along a single radial line through the origin, it gives a smooth density of the form

$$\rho(\Psi, R^2)=\frac{\pi}{R}\sqrt{\frac{2}{\lambda}}\int_0^{R^2\Psi/(R^2+\lambda)}g(E)\,\mathrm{d}E, \tag{D2}$$

and illustrates Dejonghe's (1986, section 1.2) point that $\rho$ can be much better behaved than $f$. We shall now show how to recover the distribution function (D1) from the density (D2) using our contour integral solution.

We need to impose some analyticity requirements on the function $g$, because our method requires a continuation to complex arguments. We suppose $g$ to be analytic in the circle $|E|\le 1$, which is the same as the requirement that Fricke's method needs, for a power series expansion, to converge for all physical energies. The distribution function is then given by our contour integral (B6) as

$$f(E, J^2)=\frac{|J|}{2\pi\mathrm{i}(2\lambda)^{3/2}}\frac{\partial}{\partial E}\int_0^{(E+)}\frac{\mathrm{d}\Psi}{\Psi-\Psi_0}\,g\left[\frac{J^2\Psi}{2\lambda(\Psi-\Psi_0)}\right], \tag{D3}$$

where $\Psi_0$ denotes the quantity

$$\Psi_0=E-\frac{J^2}{2\lambda}. \tag{D4}$$

The integrand of equation (D3) has a singularity at $\Psi=\Psi_0$. This lies outside the contour of integration if $\Psi_0<0$. The integrand is then analytic within the contour because of the assumed analyticity of $g(E)$, and the integral is zero. For $\Psi_0>0$, on the other hand, the contour not only encloses the singularity at $\Psi=\Psi_0$ but also the circular region in which the argument of $g$ exceeds 1 in magnitude and $g$ is not analytic. The change of variables

$$\zeta=\frac{J^2\Psi}{2\lambda(\Psi-\Psi_0)} \tag{D5}$$

is needed to handle this case. This turns the complex plane inside out and converts the integral of equation (D3) to

$$\int_0^{(E+)}\frac{2\lambda g(\zeta)\,\mathrm{d}\zeta}{2\lambda\zeta-J^2}. \tag{D6}$$

The integrand is now analytic everywhere within the contour except at the simple pole at $\zeta=J^2/2\lambda$. A simple residue calculation gives a discontinuous value of the integral and

$$f(E,J^2)=\frac{\partial}{\partial E}\begin{cases}0, & \text{if } E<J^2/2\lambda;\\ \dfrac{|J|}{(2\lambda)^{3/2}}\,g\left(\dfrac{J^2}{2\lambda}\right), & \text{if } E>J^2/2\lambda.\end{cases} \tag{D7}$$

Differentiation gives the delta function and the original $f$ of equation (D1). (The inclusion of the $E^{1/2}$ factor in equation (D1) simplifies this analysis, but it is not essential, and more general power-law branch points at $E=0$ can be handled in an essentially similar manner.)